

[RuCl₂(η⁶-*p*-cymene)(P^{*})] and [RuCl₂(κ-P^{*}-η⁶-arene)] Complexes Containing *P*-Stereogenic Phosphines. Activity in Transfer Hydrogenation and Interactions with DNA

Rosario Aznar,[†] Arnald Grabulosa,[†] Alberto Mannu,^{†,‡} Guillermo Muller,^{*,†} Daniel Sainz,[†] Virtudes Moreno,[†] Mercè Font-Bardia,[§] Teresa Calvet,[§] and Julia Lorenzo^{||}

[†]Departament de Química Inorgànica, Universitat de Barcelona, Martí i Franquès 1-11, E-08028 Barcelona, Spain

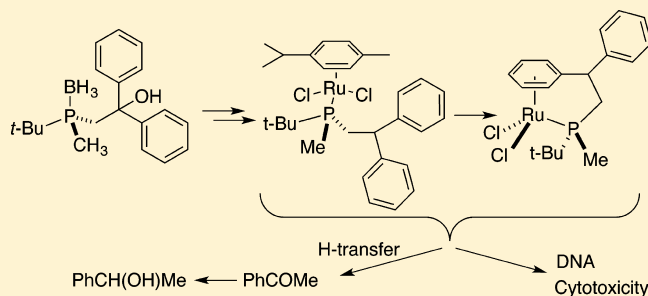
[‡]Istituto di Chimica Biomolecolare, CNR, trav. La Crucca 3, 07100, Sassari, Italy

[§]Departament de Crystal·lografia, Mineralogia i Dipòsits Minerals, Universitat de Barcelona, Martí i Franquès s/n, E-08028 Barcelona, Spain

^{||}Institut de Biotecnologia i de Biomedicina, Universitat Autònoma de Barcelona, 08193 Bellaterra, Barcelona, Spain

S Supporting Information

ABSTRACT: The preparation of a series of half-sandwich ruthenium complexes, [RuCl₂(η⁶-*p*-cymene)(P^{*})] (P^{*} = *S*-PMeRR') and [RuCl₂(κ-P^{*}-η⁶-arene)], containing *P*-stereogenic phosphines is reported. The borane-protected *P*-stereogenic phosphines have been obtained by addition of the (H₃B)PMe₂R (R = *t*-Bu (1), Cy (2), Fc (3))/*sec*-BuLi/(−)-sparteine adduct to benzyl halides, carbonyl functions, and epoxides with yields between 40 and 90% and ee values in the 70–99% range. Those containing an aryl secondary function have been used in the preparation of [RuCl₂(η⁶-*p*-cymene)-(P^{*})] complexes. Borane deprotection has been performed using HBF₄, except for (H₃B)PRMe(CH₂SiMe₂Ph) phosphines, where DABCO was used to avoid partial cleavage of the CH₂–Si bond. In the case of (H₃B)P(*t*-Bu)Me(CH₂C(OH)Ph₂) (11) the dehydrated phosphine was obtained. The tethered complexes were obtained by *p*-cymene substitution in chlorobenzene at 120 °C, except for ferrocenyl-containing complexes, which decomposed upon heating. The presence of substituents in the aryl arm of some of the phosphines introduces new chiral elements in the tethered [RuCl₂(κ-P^{*}-η⁶-arene)] compounds. Full characterization of all compounds both in solution and in the solid state has been carried out. Crystal structure determinations of four phosphine–borane molecules confirm the *S* configuration at the phosphorus atom (1a,e,l and 2d). Moreover, the crystal structure of one *p*-cymene complex (5i) and four tethered complexes reveal the strain of the compounds with two atoms in the tether (7c,g,l and 8i). Tethering has a marked effect on the catalytic performance transfer hydrogenation of acetophenone and on the nature of hydridic species originating during the activation period. The chiral induction attains 58% ee with complexes with the bulkiest substituents in the pendant arm of the phosphine. Three of the prepared complexes can interact with DNA and present a reasonable cytotoxicity toward cancer cells. Intercalation of the free aromatic pendant arm of the phosphines seems to be fundamental for such interactions.



INTRODUCTION

The chemistry of η⁶-arene ruthenium complexes has received considerable attention in recent years, since a large number of applications in catalysis,^{1,2} supramolecular chemistry,³ and medicinal chemistry⁴ have been developed with excellent or promising results. The usual pseudotetrahedral three-legged piano-stool structure of the Ru(II) complexes opens the possibility of modifying the nature of each of the four ligands, giving neutral or ionic complexes. Furthermore, chirality can be introduced through the ligands or even at the ruthenium center, which becomes stereogenic when all ligands are different.⁵ One way to introduce an initial stereogenic center is using a *P*-stereogenic phosphine in [RuCl₂(η⁶-*p*-cymene)(P^{*})] arene complexes. When the phosphine contains an appropriate aryl

pendant arm, it is possible to obtain the tethered [RuCl₂(κ-P^{*}-η⁶-arene)] compounds. If the aryl pendant arm contains suitable substituents, it is possible to introduce different new elements of chirality in the tethered complex.

In electronically saturated metal complexes it is expected that the first step of almost any metal-mediated process must be the total or partial dissociation of ligands to form free coordination positions.⁶ In arene complexes [RuCl₂(η⁶-*p*-cymene)(P^{*})] the use of basic trialkylphosphines disfavors their dissociation in comparison with triarylphosphines. Chiral phosphino–arene tethered ruthenium complexes present a more rigid and less

Received: December 19, 2012

labile environment around the metal center in comparison with the nontethered counterparts, a feature that could be particularly useful in order to use these compounds for the discrimination of prochiral substrates in catalytic organic synthesis.⁷

Moreover, the polydentate nature of the κ -P*- η^6 -arene ligand could also increase the usual low isomerization barriers of racemization in the chiral ruthenium–arene intermediates.⁸

In a previous communication⁹ we explored this synthetic approach using *P*-stereogenic phosphines obtained by the methodology developed by Muci and Evans.¹⁰ In the present work we have extended the study in two aspects: the design of appropriate potentially bidentate phosphino–arene and phosphino–pyridine ligands and the use of some of these chiral phosphino–arene ligands in the preparation of arene–ruthenium complexes in order to evaluate differences between tethered and nontethered complexes in catalysis and in their interactions with DNA.

RESULTS AND DISCUSSION

Preparation of the Phosphine–Borane Adducts by Desymmetrization of Dimethylphosphines. Several methods to prepare optically pure *P*-stereogenic phosphines have been developed using different approaches.¹¹ In particular the synthetic potential of lithium salts of carbanions stabilized by coordination to chiral ligands such as (–)-sparteine has been known for some time¹² and even the crystal structures of some of these salts have been determined.¹³ The application of this type of asymmetric deprotonation to the synthesis of *P*-stereogenic phosphines, originally proposed by Muci and Evans,¹⁰ is one of the most successful achievements of that methodology. Since the first report, the procedure has been successfully applied to the synthesis of many families of *P*-stereogenic mono- and diphosphines.¹⁴

To improve the Evans methodology of desymmetrization of prochiral substrates, a number of sparteine surrogates have been developed to overcome the limitation of the availability of only one enantiomer of sparteine and its limited supply.^{14b,15} Here we expand our initial communication on the application of this methodology to the synthesis of *P*-stereogenic phosphines containing an aromatic pendant arm able to form tethered arene ruthenium complexes or potentially act as bidentate or tridentate ligands.

To explore the scope of the Evans methodology, dimethyl-(*tert*-butyl)phosphine–borane (**1**) was initially used as the prochiral dimethylphosphine model for all reactions with different electrophiles, but subsequently another two protected dimethylphosphines (**2**, **3**) were also tested to evaluate the role of the third substituent (Chart 1). Previously reported phosphine–borane adducts of this kind by us^{9,16} or others^{17a,b} are depicted in Chart 2.

The deprotonation reaction was carried out using *sec*-BuLi/(–)-sparteine in a 1/1 ratio at low temperature. Three hours later the electrophile was added. Benzyl bromides or silyl halides (Schemes 1–3), ketones or aldehydes (Scheme 4), and

epoxides (Scheme 5) were used as electrophiles. To ensure high enantioselectivities, the reactions must be performed at –78 °C, and only after the addition of a slight excess of electrophile the temperature can be allowed to reach room temperature very slowly. A possible excess of lithium species as the temperature increases could produce side deprotonation reactions of the second methyl group or in the methylene links, decreasing the overall yield, as observed by O'Brien.¹⁸ Conversions that could reach 90% were achieved with *t*-Bu phosphines, but those containing the ferrocenyl or cyclohexyl groups only reached around 60% conversion according to ³¹P NMR spectra of the crude products. Since the reactivity of organolithium reagents is increased by coordination to (–)-sparteine, O'Brien envisaged the possibility of using substoichiometric amounts of the chiral auxiliary and developed ligand-accelerated asymmetric deprotonations,¹⁷ but in order to obtain the best enantioselectivities, the ratio RLi/(–)-sparteine was kept stoichiometric or with a slight excess of (–)-sparteine. Direct dilithiation of (BH₃)PPhMe₂ was recently reported by Strohmam, who used the diamine (*R,R*)-TMCD and *t*-BuLi for the deprotonation reaction, but this reaction was not observed under our conditions.¹⁹

The use of *meta*-substituted benzyl halides is convenient in order to introduce a second element of chirality in the metal-tethered complexes. Another important modulation of the pendant arm of the phosphines is the selection of the length of the chain between the phosphorus atom and the aromatic moiety. Direct substitutions on benzyl bromides gave yields in a satisfactory range (35–90% estimated by ³¹P NMR of the reaction solution), but this was not the case when the number of carbon atoms increased between the aryl and bromide groups (**1h**). To improve the reproducibility and yields in the preparation of phosphines containing longer arms, nucleophilic substitution was performed on appropriately substituted chlorosilanes (Scheme 2). With these electrophiles, a group of phosphines with spacers of three (**i**) and two atoms (**j**) for a comparison of their coordination behaviors was obtained in excellent yields (Scheme 3).

When chlorodimethyl(phenyl)silane was used as electrophile (**j**), the methylenic group that is initially formed after the electrophilic attack on the carbanion is sufficiently acidic to compete with the methyl group of another molecule of the starting material and suffers a second deprotonation. To minimize this side reaction, a very slow increase of the temperature upon addition of the electrophile is crucial. The phosphine–borane **1j** has been described previously but has not been further developed.^{17a,b}

The reaction of the lithium carbanion with carbonyl compounds is very efficient, giving quantitative yields and good enantioselectivities on the obtained phosphines. Livinghouse, Kann, and O'Brien used benzophenone for quenching the lithium complex of prochiral phosphine–boranes with different chiral dinitrogen auxiliaries as a method to evaluate the enantioselectivities achieved.^{14b,15a–c,17a,b,20} Indeed, **II** was obtained but its deprotection was not described. We explored the reaction with other three different carbonyl reagents, which included one or two pyridine rings: benzopyridyl ketone, dipyrindyl ketone and pyridylaldehyde (Scheme 4).

Livinghouse²¹ developed an effective route to optically pure secondary phosphine–boranes (*R*)-(BH₃)PPhHMe from (BH₃)PPhMe₂. We have reproduced the preparation of compound **II'**, precursor of the secondary phosphine, with

Chart 1

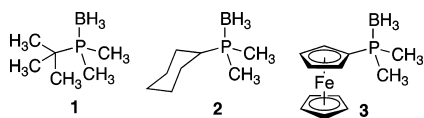
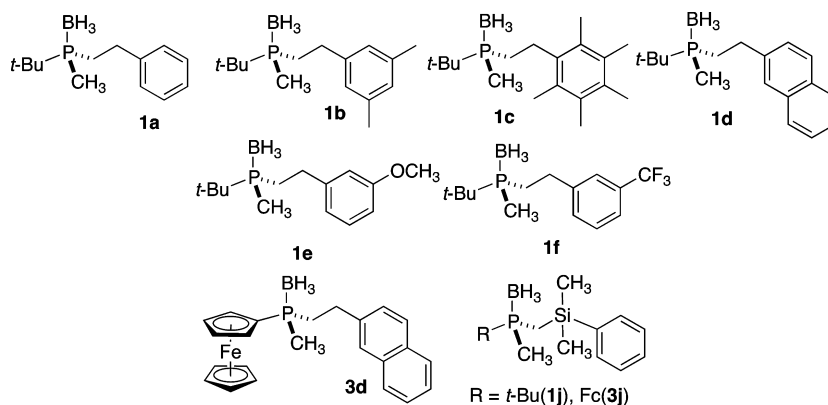
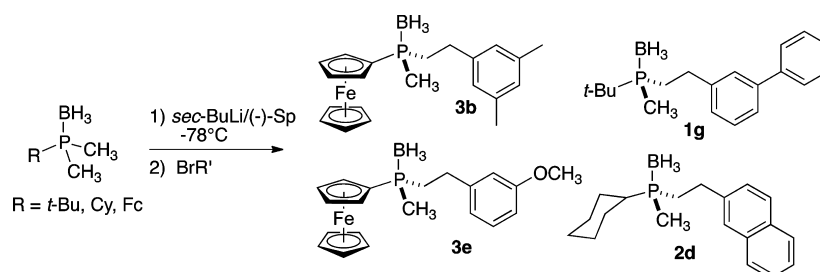


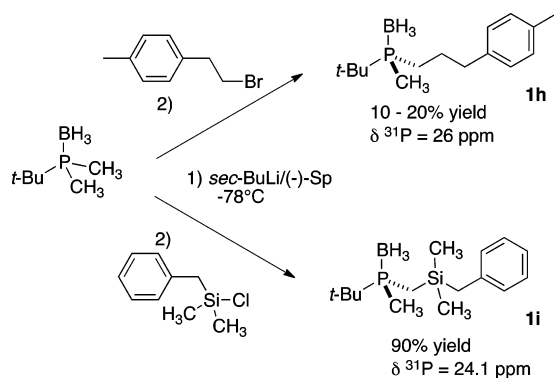
Chart 2



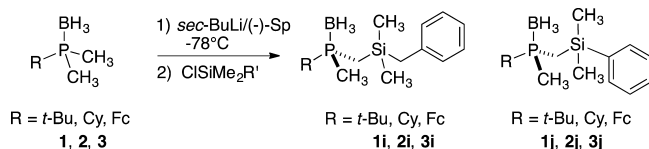
Scheme 1



Scheme 2



Scheme 3



the same excellent yields. The preparation of phosphine–borane **11''** confirms the previous formation of the alcohol.

In the preparation of adducts **1k,m** a new stereogenic carbon atom was created but no diastereoselection was observed, since the two possible diastereomers, S_P,S_C and S_P,R_C , were formed in the same amounts and they could be separated and isolated by flash chromatography.

Other functionalities susceptible to nucleophilic attack are epoxides, which upon opening lead to phosphino–alcohols. The reaction with styrene oxide takes place with good

conversion (80%) and with complete regioselectivity of the nucleophilic attack at the secondary carbon of the oxirane ring (Scheme 5). When racemic styrene oxide was used, the two diastereomers (S_P,S_C and S_P,R_C) were obtained, but using optically pure styrene oxide allowed the isolation of a single diastereomer. In this example (*R*)-styrene oxide has been used to characterize **1p** (S_P,R_C).

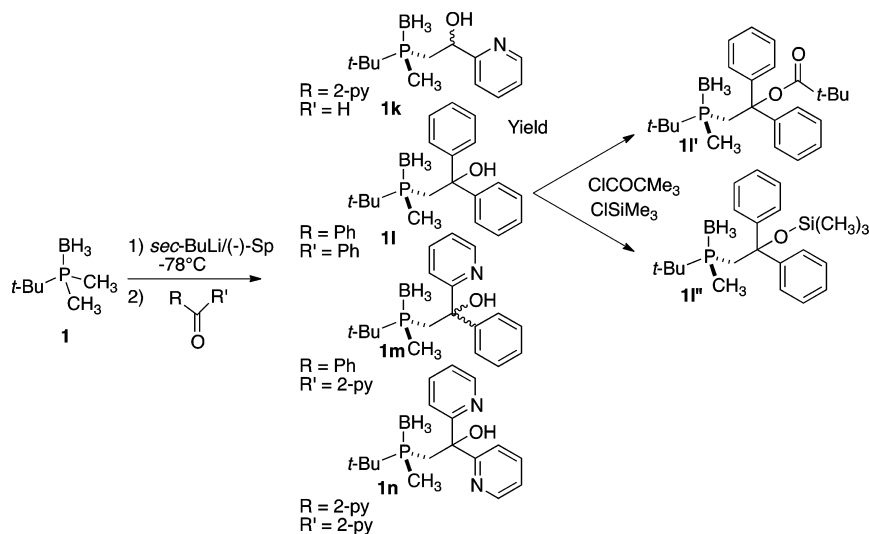
The new phosphine–boranes obtained were characterized by means of elemental analysis, infrared spectroscopy, NMR spectroscopy, HPLC analysis, and polarimetry (see the Supporting Information). In some cases, their absolute configuration was confirmed by a crystal structure determination.

HPLC analyses have allowed the evaluation of the optical purity of the phosphine–boranes. In general, the ee has been found to be higher than 95% after workup and purification (Table 1). Phosphine–boranes obtained from silyl chlorides and those containing the ferrocenyl substituent showed reduced ee's, as observed by Kann.^{14c} Jamison reported that monodentate chiral ferrocenylphosphines prepared from the ephedrine-based oxazaphospholidine–borane complex were obtained with better than 95% ee values in most cases.²²

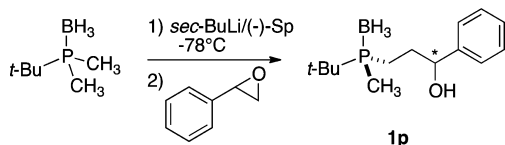
³¹P NMR spectroscopy of phosphine–borane adducts showed a single broad quartet due to the coupling to the ¹¹B atom (Table 1). The two diastereomers of **1k** could be separated by flash chromatography and were observed at 22.45 and 25.27 ppm. The diastereomeric mixture of **1m** appeared as a broad signal at 20.20 ppm. The chemical shifts of the phosphine–boranes spanned a narrow range of values for each group of compounds **1**, **2**, or **3**, with those of the ferrocenylphosphine adducts (**3**) appearing at lower fields.

¹H spectra at room temperature did not show any remarkable particularities, except for the duplicity of the signals of the

Scheme 4



Scheme 5



hydrogen atoms belonging to the methylene or dimethylsilyl linkers of the pendant arm due to their diastereotopic character. The pattern is complicated when the chain between the phosphorus atom and the aryl moiety is an ethylene group, since the spin system is a five-nucleus AA'BB'X. The signals of the CH₂Ar methylene appeared at lower fields than those of CH₂P methylene. In the rest of the adducts, assignments were possible using 2D HSQC experiments and taking into account the different contributions of the coupling constants to the ³¹P

nucleus, although with frequently overlapped signals. Accordingly, doublets of doublets or pseudotriplets could appear for each proton of the methylene group bound to the phosphorus atom, a doublet for each proton of the methylene group bound to the aryl moiety in the adducts i and two singlets for the SiMe₂ linker in adducts i and j.

¹H and ¹³C NMR spectra of the phosphine–borane 3 showed a similar pattern for the signals of the cyclopentadienyl rings of the ferrocenyl substituent: one single peak for the unsubstituted Cp ring and a group of more or less overlapped signals for the Cp–P ring, in which all atoms are different, reflecting the lack of symmetry in the phosphine–borane adduct.

The molecular structures of some of the borane-protected phosphines were determined by single-crystal X-ray analysis to confirm the absolute configuration of the obtained enantiomer. Bond distances and angles are similar to those previously

Table 1. Relevant Data of Selected Phosphines and Different Adducts Obtained by Stereoselective Deprotonation of BH₃PMe₂R (R = *t*-Bu (1), Cy (2), Fc (3))^a

	P–BH ₃ ee (<i>S</i>), %	δ(³¹ P) P–BH ₃ q (<i>J</i> _{PB})	δ(³¹ P) free P	δ(³¹ P) P–Se d (<i>J</i> _{PSe})	δ(³¹ P) P–H ⁺ d (<i>J</i> _{PH})
1a ⁹	99	25.0 (60)	–15.5		
1b ⁹	90	24.9 (57)	–15.7	48.8 (697)	
3b	98	6.20 (58)	–46.2	21.6 (709)	
1c ⁹	99	24.9 (57)	–14.4	48.3 (693)	
1d ⁹	99	25.2 (55)	–15.3	49.0 (692)	
2d	98	15.40 (75)			
3d ¹⁶	99	2.01 (62.2)	–46.1	21.8 (710)	
1e ⁹	99	25.2 (57.4)	–15.5		
3e	82	6.8 (73)			
1f	99	27.4 (54)	–15.4		
1g	99	27.1 (52.0)	–15.4		
1i	82	24.1 (59.7)	–23.4	41.2 (683)	4.64 (470)
2i	75	14.0 (61.7)	–36.6	29.3 (678)	4.70 (475)
3i	70	4.26 (60.6)	–51.5	14.4 (697)	0.80 (502)
1j ^{-16,17a}	99	24.0 (68.8)	–23.2	39.5 (705)	
2j	84	14.7 (60.4)	–36.8	27.8 (702)	
3j ¹⁶	82	4.59 (57.7)	–52.1	12.8 (722)	
1l	99	20.2 (62.4)	–19.2		
1p (<i>S</i> _p , <i>R</i> _C)	86	26.0 (69.0)			

^aee values were obtained by HPLC with a Chiracel OD-H column. ³¹P NMR spectra (inset of acetone-*d*₆, 298 K, 101 MHz, δ in ppm, *J* in Hz).

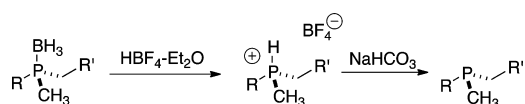
reported for related *P*-chiral phosphines (Figure 1S and Table 1S in the Supporting Information).²³ In all structures the stereogenic phosphorus atom had an *S* configuration, as expected.

Deprotection of the Phosphorus–Borane Adducts.

Borane protection can be removed by different protocols. For arylphosphine–borane adducts amines such as morpholine and diethylamine are commonly used, and when secondary amines are not compatible with some functional groups present in the starting adduct, a tertiary amine such as DABCO is a good option.²⁴ Even the use of polymer-supported amines has been reported.²⁵ For trialkylphosphine–boranes the use of strong acids with a weakly coordinating, nonoxidizing conjugate base such as $\text{HBF}_4 \cdot \text{Et}_2\text{O}$ is more convenient.²⁶ The use of alcohols with or without molecular sieves to perform the deprotection has been proposed, but only for phosphine adducts containing at least one phenyl group attached to the phosphorus atom. We have verified this extreme.²⁷

Given the electron-rich character of all the phosphine–boranes synthesized in this work, the strong acid deprotection method was used to attain the free phosphine (Scheme 6).

Scheme 6. Removal of the Borane Unit by $\text{HBF}_4 \cdot \text{Et}_2\text{O}$ ^a

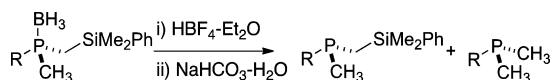


^aThe deprotection is complete after 1 h for all of the substrates.

Initially the addition of $\text{HBF}_4 \cdot \text{Et}_2\text{O}$ to a solution of the phosphine–borane in CH_2Cl_2 led to the formation of the protonated phosphine $[\text{HP}^*]^+$, which in a second step was converted into the corresponding free phosphine by addition of a degassed aqueous solution of NaHCO_3 . The deprotection process was monitored by ^{31}P NMR. One advantage of this methodology is that the protonated phosphine is indefinitely stable, even in contact with air. This operation was performed with the phosphine adducts that were used to explore their coordination to ruthenium.

Deprotection by $\text{HBF}_4 \cdot \text{Et}_2\text{O}$ showed a limitation with some phosphine adducts, since for the products **1j**, **2j**, and **3j** variable amounts of the starting dimethylphosphine were recovered (Scheme 7).

Scheme 7. Deprotection of Phosphines **1j**, **2j**, and **3j**



The combination of the stabilizing effect of the phenyl ring directly connected to the silyl fragment and the high affinity between silicon and fluoride led to the elimination of the silyl unit with consequent formation of dimethylphosphine after neutralization. This kind of behavior is not new; O'Brien took advantage of it by using the dimethylphenylsilyl moiety as a protecting group for the methyl group in *tert*-butyldimethylphosphines.¹⁸ To overcome this limitation, adducts **1j**, **2j**, and **3j** were deprotected using DABCO in hot toluene. Another side reaction was the elimination of the $-\text{OH}$ group of **1l** when it was deprotected in acidic media, a fact confirmed after preparation of the ruthenium complex. The abstraction of OH could be favored by the charge stabilization due to the presence

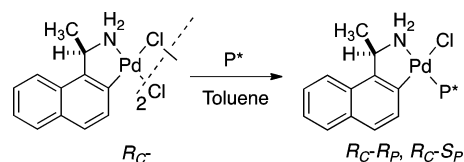
of two phenyl groups; the proton of the final $-\text{CHPh}_2$ fragment could be abstracted from the borane decomposition products. The other phosphine–borane coming from the addition over $\text{C}=\text{O}$ double bonds, potentially bidentate PN ligands, were not deprotected.

Free phosphines were very easily oxidized and therefore were immediately coordinated with ruthenium or converted to the selenides to avoid decomposition.

To confirm that the deprotection of the phosphine–boranes retained the original optical purity, the diastereomeric ratio of the product of the reaction between the free phosphine and a chiral dinuclear cyclopalladated complex was evaluated. This known fast methodology uses ^1H or ^{31}P NMR spectroscopy to roughly assess the enantiomeric purity of the phosphine.²⁸

Palladium cyclometalated complexes derived from (*R*)-1-(1-naphthyl)ethylamine have been prepared as chiral derivatizing agents to perform this kind of control (Scheme 8).²⁹

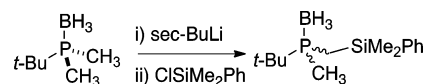
Scheme 8



If ^{31}P NMR signals corresponding to the two diastereomers have different enough chemical shifts, it is possible to evaluate the diastereomeric ratio of the mixture from the relative areas of the signals. Alternatively, the same measurement could be performed using the methyl signal of the cyclometalated ligand in the ^1H NMR. This ratio reflects the enantiomeric excess of the original mixture of the starting phosphine.

To check this methodology, the phosphine–borane **1i** in racemic form was prepared using the same standard procedure without addition of (–)-sparteine (Scheme 9).

Scheme 9. Synthesis of Phosphine–Borane **1i** in Racemic Form



The ^{31}P spectra of the corresponding cyclometalated palladium complexes with deprotected phosphine–borane *rac*-**1i** and *S*-**1i** obtained with the (–)-sparteine methodology are depicted in Figure 1, showing that it is possible to evaluate the enantiomeric purity of the free phosphine obtained after the deboration (ratio close to 9/1). The same verification was performed with **2d** (~99% ee), **3d** (~99% ee), and **3i** (~65% ee), giving results roughly similar to those obtained by HPLC of the protected phosphines.

Comparison of the σ -Donating Power between Phosphines. The influence of the substituents on the phosphorus lone pair in a phosphine is a combination of electronic and steric factors. Electron-withdrawing groups increase the *s* character of the lone pair of the phosphine, while bulky substituents widen the intervalence angles and reduce the *s* character of the phosphorus lone pair.^{30,31} Therefore, an experimental comparison of the σ -donating ability of phosphines surrounded by different substituents must be referred to the selected acceptor. Tolman³² used a carbonyl

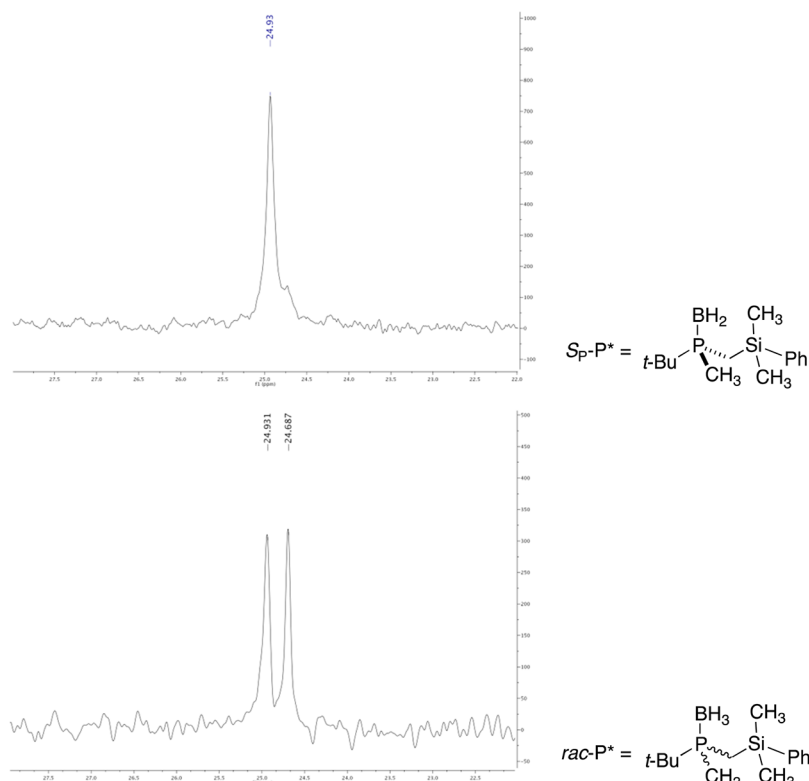
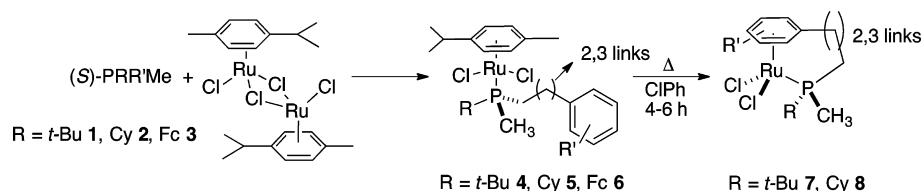


Figure 1. ^{31}P NMR spectra of the cyclopalladated complex with phosphine **1i** prepared with the standard (–)-sparteine methodology or in racemic form. A solution of the deprotected phosphine in CH_2Cl_2 was added to a solution of the cyclopalladated dimer in CH_2Cl_2 .

Scheme 10. Synthesis of Ruthenium Complexes



nickel complex to perform this kind of evaluation, but another way to perform this comparison is to use the magnitude of $^1J_{\text{PX}}$, where X should ideally be a nucleus with $S = 1/2$. Selenium is an excellent candidate, since it contains a 7.58% of the isotope ^{77}Se with $S = 1/2$ and the phosphine–selenides can be easily obtained by direct reaction between selenium or SeCN^- and the free phosphine.^{31,33} The results collected in Table 1 were obtained from phosphine–selenides prepared by overnight stirring of the corresponding deprotected phosphines with elemental selenium in toluene at room temperature or with gentle heating. The $^1J_{\text{PSe}}$ values were obtained from satellites of the ^{77}Se isotopologue present in the spectra of the corresponding phosphine–selenides; no further characterization was attempted. The values obtained are in the range reported for these kinds of phosphines (PPh_3 , 728.9 Hz;³¹ PPh_2Fc , 731.1 Hz;³¹ $\text{P}n\text{Bu}_3$, 689 Hz;³⁴ PCy_3 , 672.9 Hz;³¹ PtBu_3 , 693 Hz;³⁵ PtPr_3 , 696 Hz³⁵). The $^1J_{\text{PSe}}$ values increase with the s character of the lone pair, reflecting a decrease in the basicity of the phosphine.

The data in Table 1 show some interesting features; in phosphines with the same primary substituent R ($\text{PMeR}(\text{CH}_2\text{R}')$, **1–3**), the order of σ basicity is $t\text{-Bu} \approx \text{Cy} > \text{Fc}$ (see series **i** and **j**), a trend also observed for the prochiral

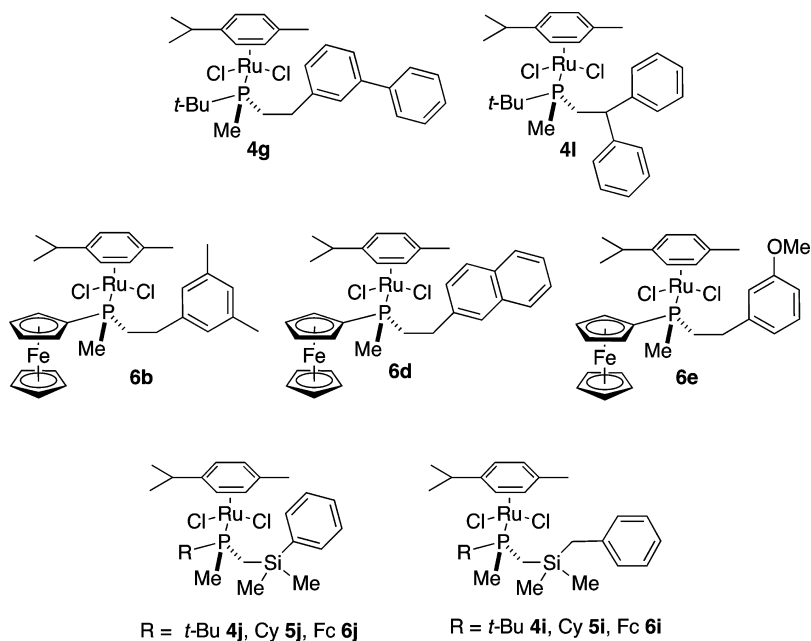
phosphines $\text{SePMe}_2(t\text{-Bu})$ and SePMe_2Fc ($\delta(^{31}\text{P})$ 39.2 ($J_{\text{PSe}} = 690$ Hz) and 11.5 ($J_{\text{PSe}} = 702$ Hz), respectively).

The change of the group R' in the pendant arm of the phosphine is also reflected in $^1J_{\text{PSe}}$. The most significant difference, probably for steric reasons, was observed when comparing the remote $-\text{SiMe}_2\text{Ph}$ group (**3j** for instance) with the more basic $-\text{SiMe}_2\text{CH}_2\text{Ph}$ (**3i**).

Since it is necessary to monitor the formation of the phosphonium salts $[\text{P}^*\text{H}]^+$ by $^{31}\text{P}\{^1\text{H}\}$ NMR spectroscopy in the first step of the deprotection of the phosphine–borane adducts in acidic media, it is possible to record the same spectra without proton decoupling. The values of $^1J_{\text{PH}}$ obtained with the adducts **1i–3i** (Table 1) showed a trend similar to that obtained from the $^1J_{\text{PSe}}$ coupling constants, suggesting that $^1J_{\text{PH}}$ values could be used for the same comparative purposes with the minimum possible steric distortion.

Preparation of Ruthenium Complexes. A group of $[\text{RuCl}_2(\eta^6\text{-}p\text{-cymene})(\text{P}^*)]$ (P^* = deprotected phosphine) complexes was synthesized by reaction of the dimeric p -cymene ruthenium precursor and the appropriate pure deprotected phosphines containing a pendant arm potentially capable of stabilizing a polydentate $\kappa\text{-P}^*\text{-}\eta^6\text{arene}$ ligand. Ruthenium-tethered complexes were obtained through an intramolecular arene substitution reaction by heating the

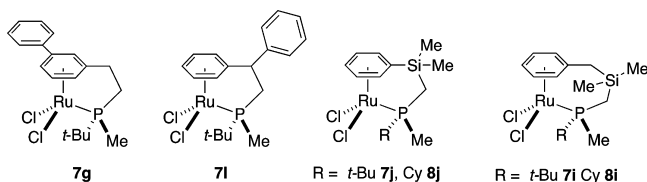
Chart 3. New Open Complexes Obtained



complexes $[\text{RuCl}_2(p\text{-cymene})(\text{P}^*)]$ ($\text{P}^* = \text{tert}$ -butyl- and cyclohexylphosphines) in chlorobenzene at 120°C (Scheme 10).³⁶ The ferrocenyl-containing phosphines were thermally unstable under these conditions, and even the use of $[\text{RuCl}_2(\text{benzene})(\text{P}\text{-ferrocenyl})]$ complexes as starting materials was unsuccessful. Attempts to prepare the ferrocenyl-tethered complexes using $[\text{RuCl}_2(\text{DMSO})_4]$ or $[\text{RuCl}(\mu\text{-Cl})(\text{CO})_3]_2$ as starting materials were also unsuccessful (see the Supporting Information for more details). Recent examples of tethered chiral ruthenium complexes of this type have been described, in which the phosphine–arene chelates have a stereogenic center located in the bridge³⁷ or possess either planar chirality³⁸ or a stereogenic center in the phosphine substituents.³⁹ Other $\kappa^1\text{-X-}\eta^6\text{-arene}$ complexes containing nitrogen, oxygen, sulfur, or carbene coordination arms are also known.⁴⁰

Elemental analyses and ^{31}P , ^1H , and ^{13}C NMR spectral data of all new complexes are given in the Experimental Section (Charts 3 and 4).

Chart 4. New Tethered Complexes Obtained



The nature of the different pendant arms hanging from the phosphine allowed the study of several aspects of the substitution reaction of the coordinated *p*-cymene group.

(1) When the incoming pendant arm of the phosphine contains a nonsymmetric arene moiety, namely for 2-naphthyl (d), 3-methoxyphenyl (e), and 3-biphenyl (g), a new element of *planar chirality* is created. NMR spectra showed the formation of diastereomeric mixtures for *tert*-butyl complexes 7e (tethered complex from $\text{PMe}(t\text{-Bu})(3\text{-MeOPh})$)⁹ (crude product $\sim 16\%$ de, isolated product 45% de) and 7g (crude

product $\sim 23\%$ de, isolated product 11% de) but only one diastereomer was detected for 7d (tethered complex from $\text{PMe}(t\text{-Bu})\text{CH}_2\text{CH}_2(2\text{-Naph})$).⁹ Careful examination of 1D and 2D NMR data confirmed that in all compounds the major diastereomer has the substituent of the coordinated aryl moiety located in an opposite position relative to the *tert*-butyl substituent of the phosphine.

(2) When the incoming phosphine contains a pendant arm with two equivalent arene groups, an additional stereogenic center is formed in the tether upon ring closure, as in the case of 7l. Once again, it is possible to evaluate the discrimination ability of the stereogenic phosphorus atom in this reaction. *tert*-Butyl and methyl substituents of phosphine I showed very limited discrimination capacity between the two phenyl groups of the pendant arm (isolated product, 5% de).

(3) The length of the linker between the phosphorus atom and the arene group is another important parameter, since the spatial disposition of the remaining phosphine substituents and the position of the substituents of the arene ligand could change as a function of the number of atoms in the linker (7i,j and 8i,j).⁴¹ Crystal structures of tethered complexes with two- or three-membered linkers are useful in evaluating the importance of these effects.

Monocrystals of sufficient quality to perform X-ray diffraction studies were obtained with the tethered complexes 7c,g described in the previous communication⁹ and 7l and 8i. Only in one case has it been possible to crystallize the open compounds (5i). The crystals were obtained by slow diffusion of hexane over a chloroform or dichloromethane solution of the complex. All complexes adopt a distorted three-legged “piano stool” geometry, showing the underlying octahedral arrangement of the different ligands. The ruthenium atom is η^6 -coordinated to the *p*-cymene or to the arene fragment of the pendant arm of the phosphine, blocking three coordination positions in the complex. The other three positions are occupied by two chlorine atoms and one phosphorus atom with angles not far from 90° between them. In complex 7c the unit cell contains two molecules that differ in the relative position of

the planes defined by the pentamethylphenyl arene and the three opposite ligands (Figure 2).

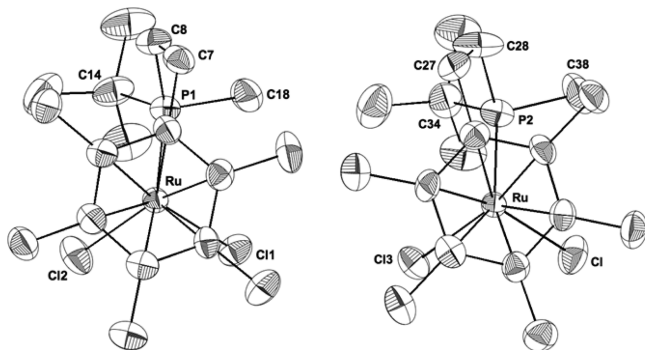


Figure 2. ORTEP drawings of the molecular structure of the two conformers of compound **7c**. Hydrogen atoms have been omitted for clarity.

Both isomers of complexes **7g** (11% de) and **7l** (5% de) were observed in solution, but the crystal used in the determination of **7g** contains only the isomer with the 3-phenyl substituent of the arene directed opposite to the *tert*-butyl group of the phosphine and **7l** is a 1/1 mixture of both isomers R_p, S_C and R_p, R_C (Figure 3). Bond distances and angles are quite similar to those reported for analogous ruthenium complexes; a selection of distances and angles is given in Table 2.⁴²

With the phosphine **2i** (*S*, 75% ee) it was possible to obtain the molecular structures of the open (**5i**) and tethered (**8i**) ruthenium complexes. In **5i** only the isomer arising from the coordination of the *S* isomer of the phosphine is present, but in the crystal there are two independent identical molecules disordered in the ratio 93/7. In **8i** the unit cell of the crystals studied contain a 1/1 mixture of the tethered complex of both isomers of the phosphine. Although it is not possible to discard completely some racemization in the thermal formation of the tethered complex, the preferred crystallization of the pairs of enantiomers seems more probable (Figures 4 and 5).

It is interesting to note that in the open *p*-cymene complexes such as **5i** and examples reported in the literature the distances arene plane–Cl and arene plane–P are similar, with a value of around 3.1 Å. In the tethered complexes, those with a chain with three-membered linkers the distances arene–P are similar, but when the chain contains two atoms in the linker the arene–

P distances decrease to around 2.8 Å without changes in the arene–Cl distances (Supporting Information). Therefore, in the solid state the claw effect of the formally tetradentate $\kappa^1-\eta^6$ ligand with the arene–phosphorus bridge containing two atoms in the linker introduces a certain tension that is also reflected in the Cl–Ru–P and Ru–P–CH₂– angles and in the slight differences in the Ru–C distances of the arene moiety, as could be observed on comparing the non trained **5i** and **8i** with complexes **7** (Figure 5 and Table 2).^{7a,c} This pincer effect does not allow us to observe differences in the distance Ru–C₆ plane when the number of methyl substituents on the arene moiety is increased: **7l** < **7b** < **7c**. The change of the spherical *tert*-butyl to the flat Cy substituents is reflected in the large differences of the Cl₁–Ru–P and Ru–P–C_R angles, where Cl₁ is directed toward R. The introduction of a silicon atom in the chain of the tethered complexes is reflected mainly in the angles C–Si–C, which are smaller than the equivalent C–C–C counterparts in analogous compounds.

All new compounds were characterized in solution by means of multinuclear NMR spectroscopy. ¹H–¹³C-HSQC and ¹H–¹H-NOESY experiments were performed to unambiguously assign ¹H NMR spectra. The position of the ³¹P, ¹H, and ¹³C NMR signals are, in general, quite similar for the phosphine ligands in complexes [RuCl₂(*p*-cymene)(P*)] containing the same substituent *t*-Bu (**4**), Cy (**5**), or Fc (**6**). The small variation is consistent with the similarity of the groups attached to the phosphorus atom (see the Experimental Section).

³¹P{¹H} NMR spectra of *t*-Bu complexes (**4**) showed a singlet around 29 ppm. The spectrum of compound **4l**, which is unique in having two phenyl groups at the β -carbon of the tether, and those containing the silicon atom in a β -position (**4i,j**) showed a slight displacement to lower field (31 and 36 ppm, respectively). The signals of the Cy complexes (**5**) appeared around 25.5 ppm, and those of the Fc series (**6**) appeared in the narrow range 9–10 ppm; in this group no effect from the silyl fragment is observed (Table 3).

To assign the proton spectra of the CH₂ groups of the pendant arm of the coordinated phosphine, it is convenient to obtain the ¹³C spectra and the corresponding HSQC. The ¹³C NMR signals of the PCH₂ and PCH₃ groups appear as doublets as a consequence of the P–C coupling, of about 20 ± 5 Hz for the PCH₂ link, 6–10 Hz lower than that observed for the PCH₃ group. The signal of the second CH₂Ar appeared in some cases as a singlet or a doublet ($J_{CP} < 4$ Hz).

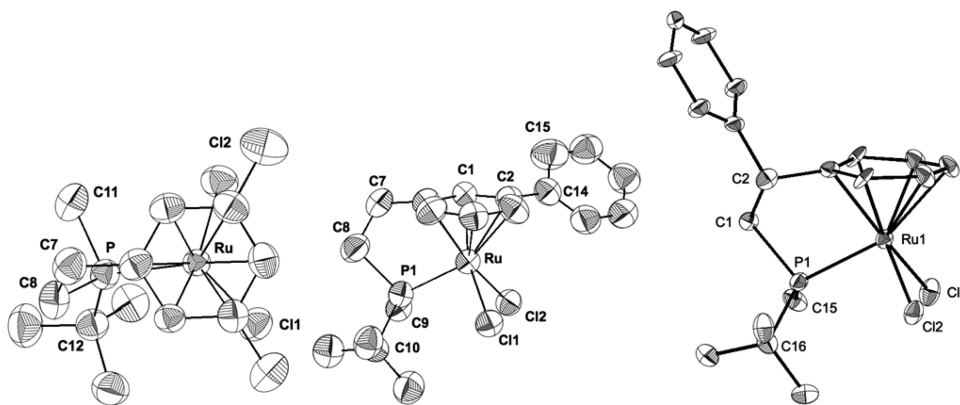


Figure 3. ORTEP drawings of the molecular structures of the ruthenium complexes **7b** (left),⁹ **7g** (middle), and the R_p, S_C isomer of **7l** (right) shown at the 50% probability level. Hydrogen atoms have been omitted for clarity.

Table 2. Selected Angles (deg) and Distances (Å) of the Tethered Complexes 7b,⁹ 7c,g,l, and 8i (with Esd's in Parentheses)

	[RuCl ₂ (η ¹ :η ⁶ -S-PMe(R)(CH ₂ R'))]				
	R = <i>t</i> -Bu (7b)	R = <i>t</i> -Bu (7c) ^b	R = <i>t</i> -Bu (7g) ^c	R = <i>t</i> -Bu (7l) ^d	R = Cy (8i)
links	2	2	2	2	3
Ru–P	2.3299(10)	2.3319(14)	2.3203(19)	2.3433(13)	2.3403(12)
Ru–Cl ₁ (R)	2.4267(13)	2.4199(17)	2.4197(17)	2.4044(14)	2.4171(12)
Ru–Cl ₂ (Me)	2.3925(13)	2.4049(16)	2.4306(18)	2.4027(10)	2.4037(12)
Ru–C ₆ plane ^a	1.694	1.698	1.707	1.693	1.702
Ru–C _{arene} chain	2.165(4)	2.141(5)	2.163(7)	2.12(2)	2.251(4)
Ru–C _{arene} <i>t</i> -chain	2.244(3)	2.271(6)	2.262(7)	2.297(14)	2.239(5)
P–CH ₂ –	1.823(4)	1.847(6)	1.924(8)	1.809(5)	1.817(5)
P–C _R	1.839(4)	1.869(7)	1.869(9)	1.850(5)	1.853(5)
P–CH ₃	1.832(5)	1.831(7)	1.777(6)	1.809(4)	1.818(5)
Cl ₁ –Ru–Cl ₂	85.61(4)	86.85(7)	86.82(6)	87.47(5)	86.71(4)
Cl ₁ –Ru–P	96.95(3)	97.39(2)	95.99(6)	96.19(5)	83.99(4)
Cl ₂ –Ru–P	88.93(4)	87.84(5)	88.73(6)	87.94(5)	90.25(4)
P–Ru–C _{arene} -chain	79.29(11)	81.17(17)	80.5(2)	81.36(5)	95.56(13)
Ru–P–CH ₂ –	104.07(14)	104.2(2)	105.5(3)	102.9(3)	115.78(15)
Ru–P–C _R	124.46(13)	124.3(2)	126.0(3)	123.20(15)	113.72(17)
Ru–P–CH ₃	112.32(16)	113.6(2)	116.0(2)	113.85(17)	114.01(14)

^aPlane defined by the six ring carbon atoms. ^bData from conformer 1. ^cThe dihedral angle between the atoms C1–C2–C14–C15 of the two phenyl planes (Ph–Ph) is 47.3°. ^dR_{P,S}C isomer.

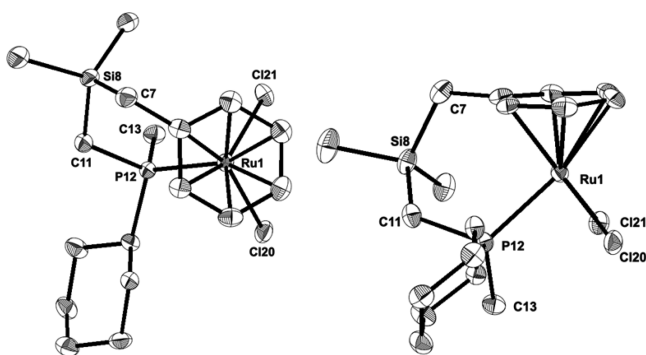


Figure 4. Molecular structure and atom-labeling scheme for the S isomer of compound 8i. Hydrogen atoms have been omitted for clarity.

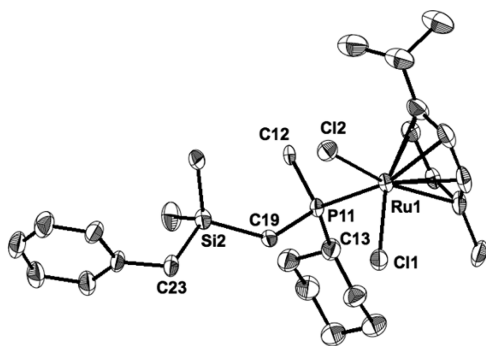


Figure 5. Molecular structure and atom-labeling scheme for compound 5i. Hydrogen atoms have been omitted for clarity. Selected bond distances (Å) and bond angles (deg): Ru1–P11, 2.350(2); Ru1–Cl1, 2.410(2); Ru1–Cl2, 2.415(2); Cl1–Ru1–Cl2, 87.34(7); Cl1–Ru1–P11, 86.59(7); Cl2–Ru1–P11, 85.49(7); Ru1–P11–C19, 115.8(3); P11–C19–Si2, 124.4(5); C19–Si2–C23, 106.2(4).

The consequence of the presence of the stereogenic phosphorus atom in the coordination sphere is the lack of any symmetry in the complex, reflected in the nonequivalence of the four CH aromatic carbons and two methyl groups of the

Table 3. ³¹P Chemical Shifts (CDCl₃, 298 K, 400 MHz, δ in ppm)

open complex	δ(³¹ P) NMR (ppm)	tethered complex	δ(³¹ P) NMR (ppm)
4g	29.6	7g	63.6
4i	35.8	7i	32.5
4j	36.4	7j	32.9
4l	32.5	7l	47.2
5i	25.6	8i	30.2
5j	25.8	8j	32.8
6b	9.4		
6d	10.5		
6e	10.6		
6i	8.8		
6j	9.2		

isopropyl substituent of the *p*-cymene. The signals of four of the CH aromatic carbon atoms appeared between 83 and 89 ppm coupled with the phosphorus atom ($J_{PC} \approx 3\text{--}6$ Hz) and the other two at 92–94 and 107–108 ppm with few exceptions. The ferrocenyl group showed one intense signal of the carbon atoms of the free Cp in the range 68–70 ppm, but in the Cp bonded to the phosphorus atom it is possible observe up to four signals in the range 68–72 ppm coupled with the phosphorus atom ($J_{PC} \approx 6\text{--}10$ Hz), although they are overlapped in some complexes.

In the ¹H NMR spectra the signals of the phosphine protons of the PMe and the P(*t*-Bu) moieties are observed between 1.00 and 1.60 ppm as two doublets. The cyclohexyl protons are dispersed between in the 1–2 ppm range and those of the ferrocenyl fragment appeared divided for the two Cp rings, near 4.15 ppm for the unsubstituted Cp and four more or less overlapped signals for the four protons of the CpP ring in the range 4.1–4.5 ppm. The pendant arm of the phosphine showed the diastereotopic nature of the protons of the PCH₂, CH₂Ar, and SiMe₂ groups. In some complexes the pattern of the signals are complex, as expected for a AA'BB'X system; the pairs of

diastereotopic protons could reach a difference of 0.3 ppm. The CH₂Ar signal usually appears at lower field than the PCH₂ methylene signals. Finally, the signal of the protons corresponding to the noncoordinated aromatic ring of the phosphine appears in the normal range.

The signals of the *p*-cymene moiety showed the same lack of symmetry in the complex; the two methyl groups of the isopropyl substituent appeared as two doublets or a partially overlapped pseudotriplet in the range 1.2 ± 0.2 ppm, and the methyl substituent appears in the range 1.8 ± 0.2 ppm. The four CH aromatic protons appeared around 5.50 ppm; in complexes **4l** and **6i,j** four clean independent doublets are observed, but in general the signals appeared more overlapped.

In the tethered complexes **7a–f** the ³¹P chemical shift increases ~30 ppm with respect to that in the open *p*-cymene compounds **4a–f**. Complex **7g** showed the same ring contribution, but for those complexes with a silicon atom in the tether the chemical shift changed slightly up and down from the former open complexes (Table 3).

The most significant changes were observed in the ¹H NMR spectra, since the substitution of the *p*-cymene simplifies the aliphatic part and now all the arene hydrogen atoms appeared separated, showing a multiplicity of the signals according to the substituents present in the phenyl ring. The signals of the diastereotopic CH₂Ar invert the position with respect to the open complexes and appear usually at higher fields than the PCH₂ signals; the differentiation between diastereotopic protons could increase up to ~0.5 ppm, and the multiplicity remains complex except for the SiCH₂Ar methylene protons, where just a doublet appears for each proton by geminal coupling. The rigidity of the κ -P*- η^6 -arene ligand allowed observing the vicinity of the different protons of the tether and their contacts with those of the phosphine substituents and arene hydrogen atoms by NOESY experiments, some of which are depicted in the Supporting Information.

Transfer Hydrogenation. The asymmetric version of the hydrogen transfer reaction applied to the reduction of ketones has been studied in detail in recent years. The most commonly used metal catalysts are ruthenium-based complexes, usually with +II as the formal oxidation state of the Ru atom. The stabilizing ligands are a wide range of combinations between chiral polydentate nitrogen and phosphorus ligands. Arene ruthenium precursors play an interesting role, since three coordination positions located in a *fac* manner are blocked by the arene ligand, a fact that limits the numbers of possible stereoisomers. Typically, with arene ruthenium complexes, bidentate or monodentate chiral ligands have been used as fundamental partners; this has allowed the development of excellent systems for enantioselective reductions.^{1,2,4,5}

Ruthenium complexes of the type [RuCl₂(η^6 -arene)(P)] with P as a monodentate phosphorus ligand have been seldom used in the hydrogen transfer reaction, despite being stable and easy to prepare.⁴⁴ These complexes can be prepared through straightforward syntheses and give good activities in the standard hydrogen transfer reaction; they have also been tested in the asymmetric version of the reaction using chiral phosphines with some success.⁴⁵ To obtain more information about the conditions needed to improve the stability of the active species and the asymmetric induction generated by the ligand, we have tested some of the tethered and nontethered complexes in the model acetophenone reduction reaction.

In order to generate the catalytically active species, the ruthenium complexes and potassium *tert*-butoxide were

dissolved in 2-propanol and heated to reflux for 30 min, before the addition of acetophenone. This activation period was the same for all reactions.

Initially the transfer hydrogenation reactions were tested with several complexes under reflux in isopropyl alcohol (Scheme 11, Table 4). Several precursors reach almost complete

Scheme 11

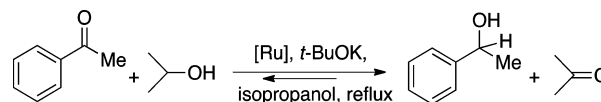


Table 4. Comparison of the Different Catalytic Precursors on the Transfer Hydrogenation of Acetophenone in Isopropyl Alcohol^a

entry	precursor	conversion at 9 h (24 h) and 82 °C, %	ee (S), %	conversion at 24 h and 40 °C	ee (S), %
1	7a ⁹	74 (97)	4		
2	7b ⁹	30 (66)	<i>rac</i>		
3	7c ⁹	23 (58)	<i>rac</i>		
4	7i			55	<i>rac</i>
5	7j			44	8
6	7d ⁹	28 (73)	23 (20)	43	50
7	8i			22	<i>rac</i>
8	8j	95	<i>rac</i>	32	<i>rac</i>
9	4c ⁹	69 (95)	8 (5)		
10	4d ⁹	36 (93)	8 (6)	42	58
11	4i			9	20
12	4j			29	<i>rac</i>
13	4l			42	59
14	5i			21	5 (R)-
15	5j	93	<i>rac</i>	6	<i>rac</i>
16	6d			15	20
17	6i			24	<i>rac</i>
18	6j			20	<i>rac</i>
19	4IH2			21	56

^a[RuCl₂(*p*-cymene)(P(*t*-Bu)MeCH₂CH₂R'))]:⁹ R' = -C₆Me₅ (**4c**), -2-Naph (**4d**). [RuCl₂(κ -P(*t*-Bu)Me- η^6 -arene)]:⁹ arene = C₆H₅ (**7a**), 2,3-Me₂C₆H₃ (**7b**), C₆Me₅ (**7c**), 2-Naph (**7d**). Conditions: substrate/catalyst/base 250/1/5, [Ru] 0.5 mM, isopropyl alcohol, after 30 min of activation.

conversion in 24 h, but the enantioselectivity was negligible, with the exception of complex **7d**, which includes a new planar element of chirality. The open [RuCl₂(*p*-cymene)(P(*t*-Bu)-MeCH₂CH₂R'))]⁹ precursors **4c** (R' = -C₆Me₅) and **4d** (R' = -2-Naph) presented higher activity than the tethered counterparts.

To check whether lowering the temperature could improve the enantioselectivity of the process, two known complexes containing (*S*)-isopropyl(aryl)phenylphosphines^{45a} and **4d** that showed a limited degree of enantioselection were tested at 40 °C (see the Supporting Information). An expected decrease of conversion and a clear increase of enantioselectivity was observed in comparison with the experiments at 82 °C. A slight evolution of ee with time could be a consequence of the ketone–alcohol equilibrium of the hydrogen transfer reaction. Therefore, in order to evaluate the discrimination ability of the ruthenium complexes, the hydrogen transfer reactions were carried out at 40 °C.

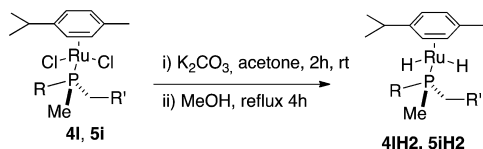
Regarding the activity, some trends were observed. The activities of the tethered precursors are lower than those of the open analogues in isopropyl alcohol at reflux; however, at 40 °C the reverse order is observed. In the group of tethered complexes in which the arene moiety presents a gradual increase in the number of methyl substituents (7a–c) the activity decreases with an increase in the number of methyl substituents on the arene, in parallel with the increase of arene basicity and steric hindrance. The presence of *tert*-butyl (4i,j), cyclohexyl (5i,j), and ferrocenyl (6i,j) substituents on the phosphine in *p*-cymene complexes or a change of the tether length from two (7j, 8j) to three atoms (7i, 8i) does not significantly affect the activity. The different basicities of *tert*-butyl- and cyclohexylphosphines with respect to ferrocenylphosphines or the increased basicity of –SiMe₂CH₂Ph-containing phosphines (i) in comparison to those containing –SiMe₂Ph (j) is not reflected in any change on the rate of the transfer hydrogenation.

With regard to the enantioselectivity, the effect of the pendant arm of the phosphines is determinant; those containing the terminal groups 2-naphthyl and –CHPh₂ in *p*-cymene or tethered complexes have significant enantiomeric excess.

The solutions containing catalytic half-sandwich precursors sometimes darken after 24 h of reaction time, which indicates decomposition of the ruthenium complex. This color change was not observed in the solutions containing tethered catalytic precursors. Similar complexes stabilized by triaryl- or diarylalkylphosphines showed reaction rates higher than those reported here with trialkylphosphines but conversely lower stability of the catalytic species.^{44c,45}

It is generally accepted that the active species in transfer hydrogenation with precursors of the type [RuCl₂(η⁶-arene)-(P*)] could be either a monohydride or a dihydride species.⁴⁶ To explore the origin of the differences observed, some tests have been performed in order to know the kind of intermediates present in solution after activation of the precursors. The position of the NMR signals of monohydride and dihydride complexes have been determined starting from the method developed by Demerseman^{46c} to directly obtain the dihydride complexes (Scheme 12). Therefore, 4IH2 and 5IH2

Scheme 12



were obtained, a single doublet is observed in the hydride region of the crude solution (4IH2, δ –12.05 ppm, $J_{\text{PH}} = 42.5$ Hz; 5IH2, δ –10.38 ppm, $J_{\text{PH}} = 47.5$ Hz). ³¹P{¹H} and coupled ¹³P NMR spectra showed that the amount of other species is low, confirming the nature of the main products of these reactions (see spectra of mono- and dihydride species in the Supporting Information). The CDCl₃ solutions of the dihydride complexes slowly evolve to the starting dichloride compound, and the solids obtained after concentration to dryness were used without further purification.

The dihydride complex 4IH2 was used as a precatalyst without an induction period (Table 4), showing less activity than its precursor 4I but retaining the same enantioselectivity,

pointing out that the discrimination ability of the active species does not depend on the starting complex.

To investigate the species obtained after the activation of the ruthenium complexes, 20 mL of a 0.01 M solution of [RuCl₂(*p*-cymene)(P*)] (5i) and [RuCl₂(κ -P*-η⁶-arene)] (8i) with 5 equiv of *t*-BuOK were refluxed for 30 min in isopropyl alcohol (Scheme 13). The ¹H and ³¹P spectra of the solution reaction of 5i showed the formation of several species with hydride and phosphorus signals in the range observed for mono- and dihydride complexes (Figure 6). In contrast, the solution of the reaction of 8i showed the formation of mainly a monohydride single product (Figures 7 and 8).

The results of the reduction of acetophenone can be discussed considering that the successive reaction steps must be initiated by ligand dissociation to open a free coordination position. Arene slippage or phosphine exchange are accessible initiation steps available for dihydride intermediates; exchange of the chloride ligand is also available for monohydride intermediates, although it seems less accessible as reported.^{45b} Regarding the activity, the arene and phosphine ligands in the tethered complexes must be less labile than the *p*-cymene parent complexes, but in the reactions at 40 °C the higher activity of the tethered complexes probably can be associated to the major stability of a single active species. The enantioselectivity observed is very limited, with the exceptions of the complexes bearing PCH₂CHPh₂ or PCH₂CH₂(2-naphthyl) substituents in the pendant arm of the phosphines, both tethered and in the parent *p*-cymene complexes. Furthermore, the dihydride and dichloride precursors of the same phosphine tested as catalytic precursors give similar selectivities, showing that the standard activation process leads to the same catalytically active species. These facts point toward an activation process by arene slippage or complete decoordination, as suggested for ruthenium carbene analogues.⁴⁷

Exploration of the Anticancer Activity. Since several ruthenium arene complexes showed important interactions with DNA and therefore are of pharmacological interest, two *p*-cymene complexes (5j, 6j) and one tethered complex (8j) have been used to evaluate the difference between tethered and open complexes in their interaction with DNA and possible cytotoxicity.^{4,48} The results obtained in the study of the interactions with DNA: circular dichroism and tapping mode atomic force microscopy (TMAFM) are described in the Supporting Information.

Cytotoxicity of the Ruthenium Complex against HL-60 Cells. The effect of the ruthenium complexes was examined on human leukemia cancer cells (HL-60) using the MTT assay, a colorimetric determination of cell viability during *in vitro* treatment with a drug. The assay, developed as an initial stage of drug screening, measures the amount of MTT reduction by mitochondrial dehydrogenase and assumes that cell viability (corresponding to the reductive activity) is proportional to the production of purple formazan that is measured spectrophotometrically. A low IC₅₀ value is desired and implies cytotoxicity or antiproliferation at low drug concentrations.

The drugs tested in this experiment were cisplatin and ruthenium complexes. Cells were exposed to each compound continuously for a 24 or 72 h period and then assayed for growth using the MTT end point assay. The IC₅₀ values of ruthenium complexes and cisplatin for the growth inhibition of HL-60 cells are summarized in Table 5.

The values of IC₅₀ for ruthenium complexes 5j and 6j are similar to those of cisplatin for HL-60 tumor cell lines for 72 h

Scheme 13

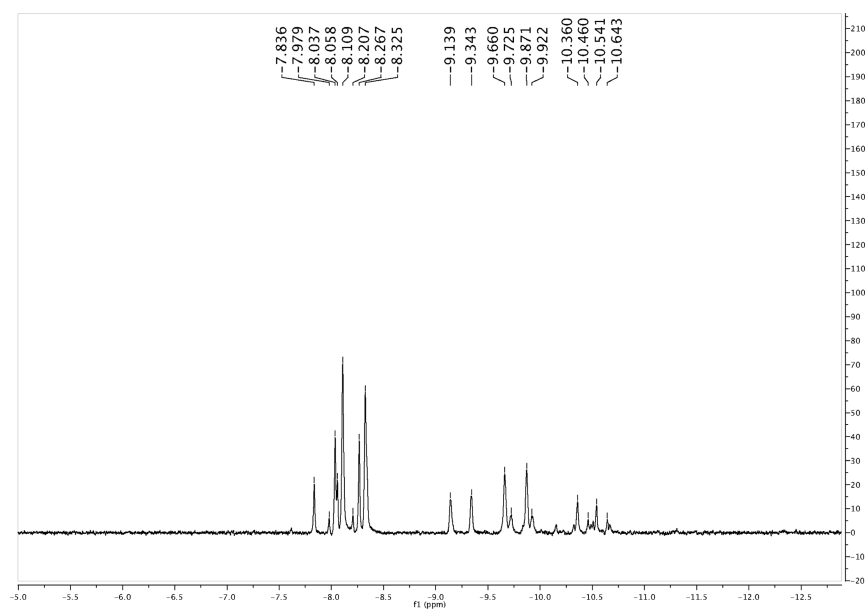
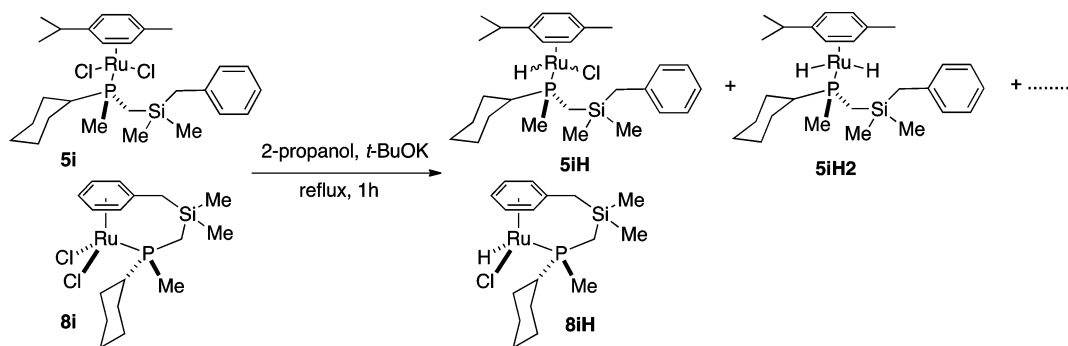


Figure 6. Hydride region of the ^1H NMR spectrum of solution of the reaction of **5i** in Scheme 13: spectrum obtained of the crude solution using an insert with d_6 -acetone at room temperature.

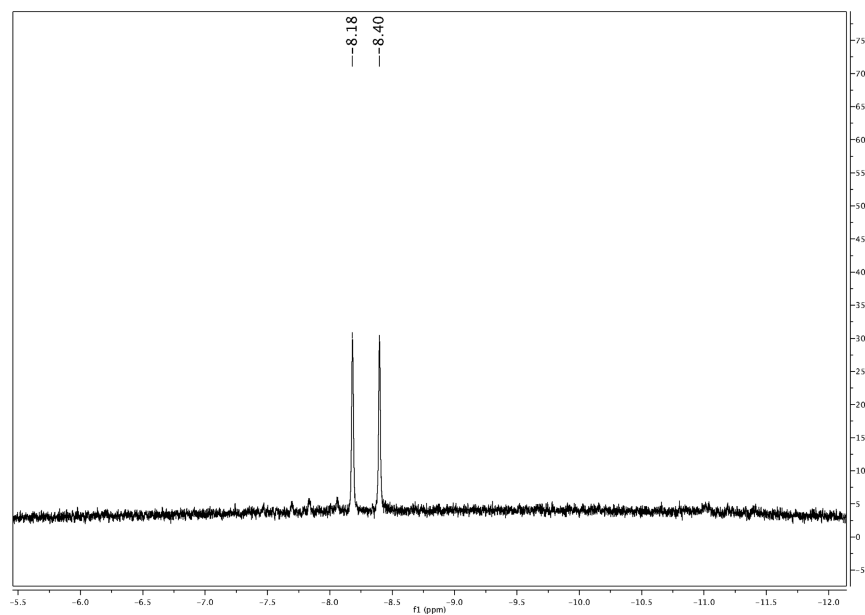


Figure 7. Hydride region of the ^1H NMR spectrum of **8iH**: spectrum obtained as in Figure 6.

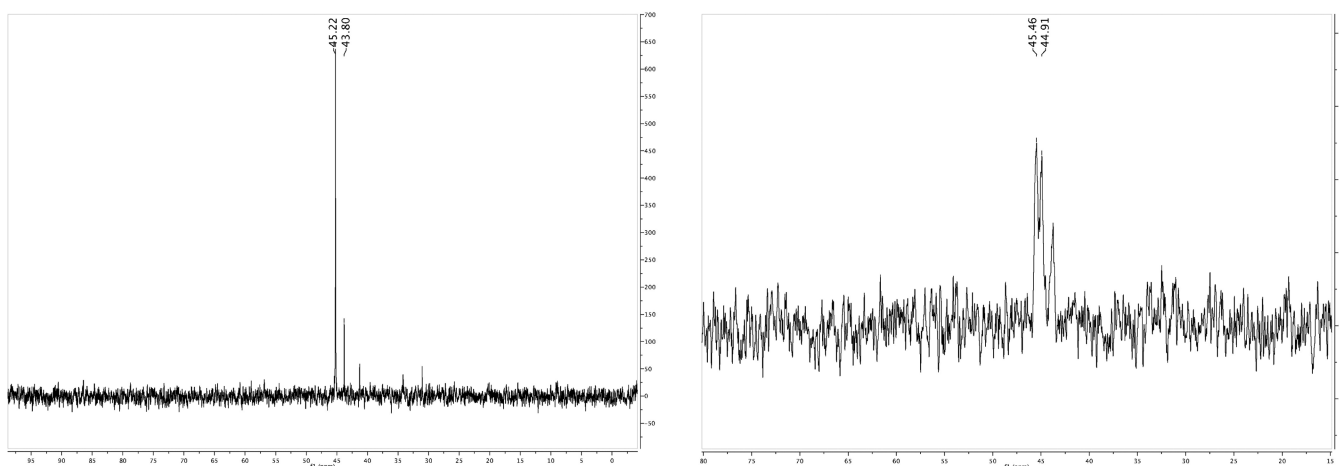


Figure 8. $^{31}\text{P}\{^1\text{H}\}$ and ^{31}P coupled NMR spectra of **8iH**: spectra obtained as in Figure 6.

Table 5. IC_{50} Values of Ruthenium Compounds and Cisplatin against HL-60 Cells

complex	IC_{50} (μM)	
	72 h	24 h
5j	3.36 ± 0.42	5.15 ± 0.29
8j	25.91 ± 4.24	52.06 ± 10.47
6j	3.72 ± 0.34	5.38 ± 0.45
CDDP	2.15 ± 0.1	15.61 ± 1.15

and lower than that of the platinum drug for 24 h. However, compound **8j** exhibits a lower activity for both 24 and 72 h of treatment.

Quantification of Apoptosis by Annexin V Binding and Flow Cytometry. We have also analyzed by Annexin V-PI flow cytometry whether ruthenium complexes are able to induce apoptosis in HL-60 cells after 24 h of incubation at equitoxic concentrations (IC_{50} values). Annexin V binds phosphatidyl serine residues, which are asymmetrically distributed toward the inner plasma membrane but migrate to the outer plasma membrane during apoptosis.⁴⁹

As can be seen in Table 6, ruthenium complexes induce cell death by apoptosis at IC_{50} treatment (29.72% for **5j**, 23.67% for

Table 6. Quantification of Apoptosis after 24 h Exposure to Concentration Equal to IC_{50} Values of Cisplatin and Ruthenium Complexes against HL-60 Cells

treatment (IC_{50} 24 h, μM)	% vital cells (R1)	% apoptotic cells (R2)	% dead cells (R3)	% damaged cells (R4)
control	92.03	2.37	5.21	0.40
CDDP (15.6)	40.18	42.77	13.88	3.16
5j (5.15)	50.75	29.72	17.81	1.73
8j (52.06)	78.45	7.71	13.03	0.81
6j (5.38)	53.67	23.67	15.02	1.38

6j, and 7.71% for **8j**). The percentages for complexes **5j** and **6j** are lower than that for cisplatin but much higher than that obtained for complex **8j**.

CONCLUSIONS

A small library of *P*-stereogenic phosphines $S\text{-PMeR}(\text{CH}_2\text{R}')$ were obtained by the Evans methodology, where $\text{R} = t\text{-Bu}$ (**1**), Cy (**2**), Fc (**3**) and R' contains an aryl, pyridyl, or alcohol functionality. The preparation of the corresponding selenides

allowed us to compare their σ -donating abilities, which were similar for **1** and **2** and more basic in comparison to **3**. Those phosphines with a pendant arm bearing a secondary aryl functionality have been selected to prepare two series of Ru(II) arene complexes. From the first series, $[\text{RuCl}_2(\eta^6\text{-}p\text{-cymene})(\text{P}^*)]$ (**4–6**), a second group of tethered $[\text{RuCl}_2(\kappa\text{-P}^*\text{-}\eta^6\text{-arene})]$ complexes (**7, 8**) have been prepared by thermal arene substitution. All phosphines and ruthenium compounds have been fully characterized both in solution and in the solid state.

When the terminal aryl fragment of the pendant arm was substituted in a nonsymmetrical way (*meta* substitution or fused aromatic rings) a new planar element of chirality was introduced when complexes **7** were prepared. The diastereoselectivity of the synthesis depends on the nature of the phosphine substituents R and R' . Within the group of complexes explored, complete diastereoselectivity was observed for $\text{R} = t\text{-Bu}$ and $\text{R}' = \text{CH}_2(2\text{-naphthyl})$. Thus, this methodology to prepare diastereomerically pure ruthenium tethered complexes seems promising, since it depends on the appropriate selection of substituents on the *P*-stereogenic phosphines.

The effect of different structural parameters of the ruthenium complexes has been evaluated in the model hydrogen transfer reduction of acetophenone. In reactions carried out at 40°C , the tethered ruthenium complexes showed better activity probably by a combination of more robustness and the presence of mainly a unique monohydride species after activation of the precursor. The enantioselectivity observed is significant when the pendant arm of the phosphine contains a bulky aryl terminus (**d, 1**) in the open or tethered catalytic precursors. The results obtained point to an arene slippage as the way to open the coordination position needed to operate the hydrogenation transfer reaction.

Some complexes were tested for potential antitumor activity against the human promyelocytic leukemia cell line HL-60 using a MTT assay. Compounds **5j** and **6j** exhibit excellent antitumor activity, with IC_{50} values similar to that of cisplatin. Compound **8j** presents a higher value for IC_{50} , being less active. The apoptotic behavior studies gave results in the same direction.

The study of the interaction of DNA with these three ruthenium compounds were carried out by CD and AFM. Results indicated modifications in tertiary ct-DNA and pBR322 plasmid DNA structures after incubation with the three

compounds, showing that DNA could be one of the targets of their antitumor mechanisms of action. The results obtained strongly suggest that the biologically active organic group is the pendant aromatic substituent available in **5j** and **6j**, but it is unavailable in the tethered complex **8j**.

EXPERIMENTAL SECTION

General Data. All compounds were prepared under a purified nitrogen atmosphere using standard Schlenk techniques. All solvents were purified by standard procedures⁵⁰ and distilled under nitrogen. ¹H, ¹³C{¹H}, ³¹P{¹H}, and HSQC ¹H–¹³C NMR spectra were recorded on Bruker DRX 250, Varian Unity 300, and Varian Mercury 400 spectrometers. NOESY spectra (¹H–¹H) were obtained on a Varian Inova 500 spectrometer. The spectra were recorded in CDCl₃ unless otherwise specified. Chemical shifts are reported downfield from standards. HPLC analyses were carried out in a Waters 717 Plus autosampler chromatograph with a Waters 996 multidiode array detector, fitted with a Chiracel OD-H chiral column. The eluent, in all determinations, was a mixture of *n*-hexane and *i*PrOH (95/5) unless otherwise noted. Optical rotations were determined with a Perkin-Elmer 241MC polarimeter at 23 °C using a sodium lamp at the sodium D-line wavelength (589.592 nm). The solvent and concentration (g/mL) for each compound are indicated in parentheses. Elemental analyses (C, H) were performed at the Serveis Científicotècnics of the University of Barcelona. The ruthenium dimers [RuCl(μ-Cl)(C₆H₆)₂] and [RuCl(μ-Cl)(C₁₀H₁₄)₂] and *tert*-butyldimethylphosphine–borane were prepared as previously described.^{14a,44a} Other reagents were used as received from commercial suppliers. The analytical results of some of the silicon-containing complexes are outside the range viewed as establishing analytical purity; they are provided to illustrate the best values obtained to date. All NMR spectra of these complexes are included in the Supporting Information.

General Procedure for Phosphine–Borane Deprotection.
Method A. A 1 mmol portion of phosphine–borane was placed in a Schlenk flask under a nitrogen atmosphere and dissolved in 10 mL of dichloromethane. The mixture was cooled to 0 °C, and HBF₄·OEt₂ (0.70 mL, ~5 mmol) was added dropwise. The solution was stirred for 30 min. The disappearance of the initial phosphine–borane signal and the presence of a new singlet corresponding to the protonated phosphine in the ³¹P NMR spectra was observed. A degassed saturated solution of NaHCO₃ (10 mL) was added, and the mixture was stirred for 1 h. ³¹P NMR confirmed the quantitative formation of the free phosphine. The organic phase was separated, dried on sodium sulfate, and filtered to obtain a solution containing the free phosphine.

Method B. A 1 mmol portion of phosphine–borane was placed in a Schlenk flask under a nitrogen atmosphere and dissolved in 10 mL of toluene. A 10 mmol portion of DABCO (1.12 g) was added, and the solution was stirred for 6 h at 90 °C. ³¹P NMR confirmed the quantitative formation of free phosphine. The solution was purified by column chromatography (alumina, toluene) to yield a solution of the free phosphine.

Half-Sandwich [RuCl₂(η⁶-arene)(P*)] Complexes. *Phosphine Deprotected with Method A.* Solid [RuCl₂(*p*-cymene)]₂ (0.31 g, 5 × 10^{−4} mol) was added to a solution containing the free phosphine, and the mixture was stirred for 30 min at room temperature. ³¹P NMR confirmed the coordination of the phosphine. The solvent was removed under vacuum, and the crude product was purified by crystallization or by flash chromatography.

Phosphine Deprotected with Method B. A solution of [RuCl₂(*p*-cymene)]₂ (0.31 g, 5 × 10^{−4} mol) in 20 mL of CH₂Cl₂ was added to the toluene solution containing the free phosphine, and the mixture was stirred for 15 min. ³¹P NMR confirmed the coordination of the phosphine. The solvent was removed under vacuum, and the crude solid was dissolved in dichloromethane. The resulting solution was washed several times with a 1 M aqueous solution of HCl to eliminate DABCO, DABCO–borane, and other derivatives. The organic phase was dried with sodium sulfate and filtered, and the crude product was purified by crystallization or by flash chromatography.

*Dichloro(η⁶-*p*-cymene)[(R)-*tert*-butyl(2-(3-phenylphenyl)ethyl)methylphosphine]ruthenium(II) (4g).* The phosphine was deprotected with method A. The preparation of this compound was carried out following the general protocol, but starting from 0.350 g (1.19 mmol) of **1g** and 0.309 g (0.50 mmol) of [RuCl₂(*p*-cymene)]₂. Yield: 0.445 g, 75%. Anal. Calcd for C₂₉H₃₉Cl₂PRu: C, 58.98; H, 6.66. Found: C, 59.1; H, 7.0%. ¹H NMR (400.0 MHz, 298 K): δ (ppm) 1.25 (d, *J* = 6.6, CH₃CH, 3H); 1.27 (d, *J* = 6.6, CH₃CH, 3H); 1.33 (d, *J*_{HP} = 13.2, (CH₃)₃C, 9H); 1.53 (d, *J*_{HP} = 10.4, CH₃P, 3H); 2.09 (s, CH₃ *p*-cymene, 3H); 2.14–2.25 (m, CH₂P, 1H); 2.49–2.60 (m, CH₂P, 1H); 2.75 (tt, *J*_{HP} ≈ *J*_{HH, gem} = 13.6, *J*_{HH} = 4.6, 1H); 2.85 (septet, *J* = 7.0, CH₃CH, 1H); 3.11 (tt, *J*_{HP} ≈ *J*_{HH, gem} = 13.5, *J*_{HH} = 4.7, 1H); 5.52 (d, *J* = 6.3, *p*-cymene, 1H); 5.58 (d, *J* = 5.9, *p*-cymene, 1H); 5.63 (d, *J* = 6.1, *p*-cymene, 1H); 5.65 (d, *p*-cymene, 1H); 7.19 (d, Ph, 1H); 7.31–7.38 (m, 2H); 7.39–7.47 (m, 4H); 7.54–7.61 (m, 1H). ¹³C{¹H} NMR (100.6 MHz, 298 K): δ (ppm) 5.8 (d, *J*_{PC} = 29.4, CH₃P); 18.1 (s, CH₃ *p*-cymene); 22.0 (s, CH₃CH); 22.6 (s, CH₃CH); 27.6 (d, *J*_{PC} = 2.7, C(CH₃)₃); 28.4 (d, *J*_{PC} = 21.6, CH₂P); 30.7 (s, CH₃CH); 31.8 (d, *J*_{PC} = 4.6, CH₂Ph); 34.7 (d, *J*_{PC} = 22.9, (CH₃)₃C); 83.0 (d, *J*_{PC} = 4.9, CH *p*-cymene); 83.6 (d, *J*_{PC} = 6.5, CH *p*-cymene); 88.2 (d, *J*_{PC} = 4.1, CH *p*-cymene); 89.9 (d, *J*_{PC} = 4.0, CH *p*-cymene); 93.2 (s, *p*-cymene); 107.8 (s, *p*-cymene); 125.1 (s, CH Ph); 126.90 (s, CH Ph); 126.95 (s, 2CH Ph); 127.2 (s, 2CH Ph); 127.3 (s, CH Ph); 129.0 (s, CH Ph); 141.1 (s, C Ph); 141.5 (s, C Ph); 142.7 (d, *J*_{PC} = 11.7, C Ph). ³¹P{¹H} NMR (101.2 MHz, CH₂Cl₂, 298 K): δ (ppm) 29.6 (s).

*Dichloro(η⁶-*p*-cymene)[(R)-*tert*-butyl(2,2-dimethyl-3-phenyl-2-sila-1-propyl)methylphosphine]ruthenium(II) (4i).* The phosphine–borane was deprotected with method A. The preparation of this compound was carried out following the general protocol. The crude orange resin was crystallized from dichloromethane/hexane to obtain the title compound as an orange powder in 90% yield. Anal. Calcd for C₂₅H₄₁Cl₂PRuSi: C, 52.44; H, 7.22. Found: C, 51.29; H, 7.34. ¹H NMR (400 MHz): δ (ppm) 0.08 (s, CH₃Si, 3H); 0.15 (s, CH₃Si, 3H); 1.01 (dd, *J* = 14.80, *J* = 13.20, CH₂P, 1H); 1.20–1.24 (m, (CH₃)₃C, CH₃CH, 15 H); 1.51 (d, *J* = 10.4, CH₃P, 3H); 1.62 (pt, *J* = 14.80, CH₂P, 1H); 1.97 (s, CH₃ *p*-cymene, 3H); 2.12 (d, *J* = 14.00, CH₂Si, 1H); 2.17 (d, *J* = 14.00, CH₂Si, 1H); 2.78 (septet, CH₃CH, 1H); 5.48 (d, *J* = 5, *p*-cymene, 1H); 5.54 (s, *p*-cymene, 2H); 5.58 (d, *J* = 5, *p*-cymene, 1H); 6.90 (d, *J* = 4, *o*-Ph, 2H); 7.02 (t, *J* = 4, *p*-Ph, 1H); 7.18 (t, *J* = 4, Ph, 1H). ¹³C{¹H} NMR (100.6 MHz): δ (ppm) −0.44 (s, CH₃Si); −0.15 (s, CH₃Si); 10.06 (d, *J* = 28.17, CH₃P); 11.01 (d, *J* = 22.14, CH₂P); 17.82 (s, CH₃ *p*-cymene); 21.91 (s, CH₃CH *p*-cymene); 22.22 (s, CH₃CH, *p*-cymene); 27.32 (s, (CH₃)₃C); 27.79 (s, PhCH₂Si); 30.47 (s, CH₃CH, *p*-cymene); 34.66 (d, *J* = 23.14, (CH₃)₃CP); 82.40 (d, *J* = 6.04, CH *p*-cymene); 83.18 (d, *J* = 6.04, CH *p*-cymene); 88.79 (s, CH, *p*-cymene); 89.53 (d, *J* = 3.02, CH *p*-cymene); 91.94 (*p*-cymene); 107.76 (*p*-cymene); 123.98 (s, Ph); 128.02 (s, Ph); 128.11 (s, Ph); 139.54 (s, Ph). ³¹P{¹H} NMR (101.2 MHz): δ (ppm) 35.8 (s). FT-IR: ν (cm^{−1}) 476; 700; 765; 828; 888; 1056; 1135; 1205; 1249; 1281; 1366; 1470; 1492; 1599; 2870; 2898; 2958; 3021; 3056.

*Dichloro(η⁶-*p*-cymene)[(R)-*tert*-butyl((dimethylphenylsilyl)methyl)methylphosphine]ruthenium(II) (4j).* The phosphine–borane was deprotected with method B. The preparation of this compound was carried out following the general protocol. The crude orange resin was crystallized from dichloromethane/hexane in order to obtain the title compound as an orange powder in 80% yield. Anal. Calcd for C₂₄H₃₉Cl₂PRuSi: C, 51.60; H, 7.04. Found: C, 51.52; H, 7.34. ¹H NMR (400 MHz): δ (ppm) 0.42 (s, CH₃Si, 3H); 0.49 (s, CH₃Si, 3H); 1.16 (d, *J* = 12.00, (CH₃)₃C, 9H); 1.20–1.24 (m, CH₂P, CH₃CH, 8H); 1.47 (d, *J* = 10.40, CH₃P, 3H); 2.01 (s, CH₃ *p*-cymene, 3H); 2.82 (septet, Me₂CH, 1H); 5.49 (d, *J* = 6.00, *p*-cymene, 1H); 5.54 (s, *p*-cymene, 2H); 5.59 (d, *J* = 5.60, *p*-cymene, 1H); 7.31–7.34 (m, Ph, 3H); 7.50–7.53 (m, 3,5-Ph, 2H). ¹³C{¹H} NMR (100.6 MHz): δ (ppm) −0.26 (s, CH₃Si); 0.41 (d, *J* = 1, CH₃Si); 9.71 (d, *J* = 29.18, CH₂P); 12.95 (d, *J* = 20.52, CH₂P); 17.84 (s, CH₃ *p*-cymene); 21.98 (s, CH₃CH); 22.27 (s, CH₃CH); 27.39 (d, *J* = 4.02, CH₃CP); 30.51 (s, Me₂CH); 34.6 (d, *J* = 6.04, CP); 82.72 (d, *J* = 5.03, CH, *p*-cymene); 83.09 (d, *J* = 7.04, CH, *p*-cymene); 88.93 (d, *J* = 4.03, CH, *p*-cymene); 89.52 (d, *J* = 3.02, CH, *p*-cymene); 92.08 (s, *p*-cymene); 107.50 (s, *p*-

cymene); 127.80 (s, Ph); 129.08 (s, 4-Ph); 133.54 (s, Ph); 139.40 (d, $J = 3.4$, 1-Ph). $^{31}\text{P}\{^1\text{H}\}$ NMR (101.2 MHz): δ (ppm) 36.4 (s). FT-IR: ν (cm^{-1}) 469; 632; 702; 783; 822; 888; 1111; 1246; 1365; 1425; 1463; 1741; 2896; 2931; 2959; 3053.

Dichloro(η^6 -*p*-cymene)[(R)-tert-butyl(2,2-diphenylethyl)methylphosphine]ruthenium(III) (4I). The phosphine was deprotected with method A. The preparation of this compound was carried out following the general protocol, but starting from 0.160 g (0.51 mmol) of **II** and 0.128 g (0.21 mmol) of $[\text{RuCl}_2(\textit{p}\text{-cymene})]_2$. Yield: 0.152 g, 61%. Anal. Calcd for $\text{C}_{29}\text{H}_{39}\text{Cl}_2\text{PRu}$: C, 58.98; H, 6.66. Found: C, 58.5; H, 6.6. ^1H NMR (400.0 MHz, 298 K): δ (ppm) 0.93 (d, $J_{\text{HP}} = 11.1$, CH_3P , 3H); 1.15 (d, $J_{\text{HH}} = 7.0$, CH_3CH , 3H); 1.22 (d, $J_{\text{HH}} = 6.9$, CH_3CH , 3H); 1.29 (d, $J_{\text{HP}} = 13.0$, $(\text{CH}_3)_3\text{C}$, 9H); 1.95 (s, CH_3 , *p*-cymene, 3H); 2.73 (septet, $J_{\text{HH}} = 7.0$, CH_3CH , 1H); 2.90–3.07 (m, CH_2P , 2H); 4.89 (m, CHPh_2 , 1H); 5.47 (d, $J = 5.9$, *p*-cy, 1H); 5.54 (d, $J = 6.0$, *p*-cy, 1H); 5.59 (d, $J = 5.9$, *p*-cy, 1H); 5.63 (d, $J = 5.9$, *p*-cy, 1H); 7.08–7.14 (m, Ph, 2H); 7.20–7.27 (m, Ph, 4H); 7.36–7.40 (m, Ph, 4H). $^{13}\text{C}\{^1\text{H}\}$ NMR (100.6 MHz, 298 K): δ (ppm) 5.1 (d, $J_{\text{PC}} = 27.8$, PCH_3); 18.0 (s, CH_3 , *p*-cymene); 21.6 (s, CHCH_3); 22.9 (s, CHCH_3); 27.8 (d, $J_{\text{PC}} = 2.8$, $\text{C}(\text{CH}_3)_3$); 30.5 (s, $\text{CH}(\text{CH}_3)_2$); 33.4 (d, $J_{\text{PC}} = 18.5$, CH_2P); 34.7 (d, $J_{\text{PC}} = 23.3$, $\text{C}(\text{CH}_3)_3$); 46.2 (d, $J_{\text{PC}} = 4.2$, CHPh_2); 82.6 (d, $J_{\text{PC}} = 4.3$, *CH p*-cymene); 84.4 (d, $J_{\text{PC}} = 6.8$, *CH p*-cymene); 87.7 (d, $J_{\text{PC}} = 4.3$, *CH p*-cymene); 90.3 (d, $J_{\text{PC}} = 3.7$, *CH p*-cymene); 107.5 (s, *C p*-cymene); 126.2 (s, CHPh); 126.3 (s, CHPh); 127.3 (s, 2 CHPh); 127.6 (s, 2 CHPh); 128.6 (s, 2 CHPh); 128.7 (s, 2 CHPh); 145.5 (s, $J_{\text{PC}} = 4$, CPh); 145.6 (d, $J_{\text{PC}} = 8$, CPh). $^{31}\text{P}\{^1\text{H}\}$ NMR (101.2 MHz, 298 K): δ (ppm) 32.55 (s). IR: ν (cm^{-1}) 3052, 3030, 2960, 2900, 2870; 1596, 1492, 1468, 1450, 1365, 922, 893, 749, 709, 535.

Dichloro(η^6 -*p*-cymene)[(R)-cyclohexyl(2,2-dimethyl-3-phenyl-2-sila-1-propyl)methylphosphine]ruthenium(III) (5I). The phosphine was deprotected with method A. The preparation of this compound was carried out following the general protocol. Monocrystals of the title product were obtained after slow evaporation from a solution of hexane/dichloromethane in 90% yield. Anal. Calcd for $\text{C}_{27}\text{H}_{43}\text{Cl}_2\text{PRuSi}$: C, 54.17; H, 7.24. Found: C, 53.41; H, 7.25. ^1H NMR (400 MHz): δ (ppm) 0.11 (s, CH_3Si , 3H); 0.13 (s, CH_3Si , 3H); 1.14 (dd, $J_{\text{HP}} = 15$, $J_{\text{HH}} = 10$, CH_2P , 1H); 1.22 (d, $J = 6.5$, CH_3CH , 3H); 1.23 (d, $J = 6.5$, CH_3CH , 3H); 1.24–1.30 and 1.76–1.94 (m, Cy, 11H); 1.48 (d, $J = 11$, CH_3P); 1.57 (pt, $J = 15$, CH_2P , 1H); 1.99 (s, CH_3 , *p*-cymene, 3H); 2.14 (s, CH_2Si , 2H); 2.78 (m, $J = 6.5$, Me_2CH , 1H); 5.40 (s, 2H, *p*-cymene); 5.46 (s, 2H, *p*-cymene); 6.96 (d, $J = 8$, 2H, *o*-Ph); 7.05 (t, $J = 8$, 1H, *p*-Ph); 7.18 (t, $J = 8$, 2H, *m*-Ph). $^{13}\text{C}\{^1\text{H}\}$ NMR (100.6 MHz): δ (ppm) –0.56 (s, CH_3Si); –0.53 (s, CH_3Si); 10.80 (d, $J = 23.14$, CH_3P); 11.08 (d, $J = 15$, CH_2P); 17.98 (s, CH_3 , *p*-cymene); 21.71 (s, CH_3CH , *p*-cymene); 22.44 (s, CH_3CH , *p*-cymene); 26.16 (s, Cy); 26.8 (d, $J = 10$, Cy); 26.9 (d, $J = 10$, Cy); 27.62 (d, $J = 3$, Cy); 28.11 (s, Cy); 28.17 (s, SiCH_2Ph); 30.46 (s, CH_3CH , *p*-cymene); 42.79 (d, $J = 25.6$, $\text{C}_{\text{C}}\text{P}$); 82.28 (d, $J = 5$, *CH p*-cymene); 84.48 (d, $J = 6$, *CH p*-cymene); 88.12 (d, $J = 3$, *CH p*-cymene); 89.67 (d, $J = 4$, *CH p*-cymene); 92.50 (s, *p*-cymene); 107.64 (s, *p*-cymene); 124.16 (s, Ph); 128.15 (s, Ph); 139.33 (s, Ph). $^{31}\text{P}\{^1\text{H}\}$ NMR (101.2 MHz): δ (ppm) 25.6 (s). FT-IR: ν (cm^{-1}) 484; 700; 763; 820; 872; 892; 918; 1116; 1203; 1250; 1448; 1492; 1598; 1637; 2850; 2924; 2957; 3022; 3050.

Dichloro(η^6 -*p*-cymene)[(R)-cyclohexyl(2-methyl-2-phenyl-2-sila-1-propyl)methylphosphine]ruthenium(III) (5J). The phosphine was deprotected with method B. The preparation of this compound was carried out following the general protocol. The crude orange resin was crystallized from dichloromethane/hexane to obtain the title product as an orange powder in 90% yield. Anal. Calcd for $\text{C}_{26}\text{H}_{41}\text{Cl}_2\text{PRuSi}$: C, 53.41; H, 7.07. Found: C, 53.62; H, 7.30. ^1H NMR (400 MHz): δ (ppm) 0.38 (s, CH_3Si , 3H); 0.45 (s, CH_3Si , 3H); 0.97–1.2 (m, Cy, 5H); 1.21 (d, $J = 5.5$, CH_3CH , 3H); 1.22 (d, $J = 5.5$, CH_3CH , 3H); 1.44 (d, $J = 12$, CH_3P , 3H); 1.46 (pt, $J = 12.5$, CH_2P , 1H); 1.83 (pt, $J = 15.3$, CH_2P , 1H); 1.65–1.95 (m, Cy, 6H); 2.01 (s, CH_3 , *p*-cymene, 3H); 2.81 (septet, CH , 1H); 5.40–5.50 (m, *p*-cymene, 4H); 7.37 (m, Ph, 3H); 7.55 (m, 3,5-Ph, 2H). $^{13}\text{C}\{^1\text{H}\}$ NMR (100.6 MHz): δ (ppm) –0.58 (s, CH_3Si); 0.15 (s, CH_3Si); 11.36 (d, $J_{\text{CP}} = 36.22$, CH_3P); 11.98 (d, $J_{\text{CP}} = 23.14$, CH_2P); 17.97 (s, CH_3 , *p*-cymene); 21.93 (s, CH_3CH);

22.25 (s, CH_3CH); 26.17 (s, Cy); 26.52 (d, $J_{\text{CP}} = 11.07$, Cy); 26.89 (d, $J_{\text{CP}} = 11.07$, Cy); 28.05 (s, Cy); 28.27 (s, Cy); 30.51 (s, Me_2CH); 42.23 (d, $J_{\text{CP}} = 26.16$, CHP); 82.52 (d, $J = 5.03$, *CH p*-cymene); 83.78 (d, $J = 6.03$, *CH p*-cymene); 88.62 (d, $J = 4.02$, *CH p*-cymene); 89.53 (d, $J = 4.02$, *CH p*-cymene); 92.17 (s, *p*-cymene); 107.73 (s, *p*-cymene); 128.01 (s, 2,6-Ph); 129.32 (s, 4-Ph); 133.61 (s, 3,5-Ph) 138.83 (s, 1-Ph). $^{31}\text{P}\{^1\text{H}\}$ NMR (101.2 MHz): δ (ppm) 25.8 (s, P-BH_3). FT-IR: ν (cm^{-1}) 472; 628; 663; 704; 743; 792; 826; 907; 1115; 1247; 1428; 1448; 1468; 2846; 2921; 3036; 3069.

Dichloro(η^6 -*p*-cymene)[(R)-ferrocenyl(2-(3,5-dimethylphenyl)ethyl)methylphosphine]ruthenium(III) (6b). The phosphine–borane was deprotected with method A. The preparation of this compound was carried out following the general protocol. The crude product was purified by flash chromatography (hexane/ethyl acetate, 9/1; $R_f = 0.27$) to obtain the title product as an orange solid in 90% yield. Anal. Calcd for $\text{C}_{31}\text{H}_{39}\text{RuCl}_2\text{PFe}$: C, 55.54; H, 5.86. Found: C, 55.76; H, 5.85. ^1H NMR (400 MHz): δ (ppm) 1.00 (d, $J = 6.80$, CH_3CH , 3H); 1.08 (d, $J = 8.00$, CH_3CH , 3H); 1.78 (s, CH_3 , *p*-cymene, 3H); 1.84 (d, $J = 11.60$, CH_3P , 3H); 2.34 (s, CH_3Ph , 6H); 2.58 (m, *CH p*-cymene, 1H); 2.60–2.73 (m, CH_2P , 2H); 3.10 (m, CH_2Ph , 2H); 4.30 (s, Cp, 5H); 4.45 (s, Cp, 1H); 4.49 (s, Cp, 2H); 4.60 (s, Cp, 1H); 5.02 (d, $J = 6.00$, *p*-cymene, 1H); 5.12 (d, $J = 6.00$, *p*-cymene, 1H); 5.16 (d, $J = 6.00$, *p*-cymene, 1H); 5.19 (d, $J = 6.00$, *p*-cymene, 1H); 6.90 (s, 4-Ph, 1H); 6.92 (s, 2,6-Ph, 2H). $^{13}\text{C}\{^1\text{H}\}$ NMR (100.6 MHz): δ (ppm) 9.18 (d, $J = 34$, CH_3P); 17.71 (s, CH_3 , *p*-cymene); 21.32 (s, CH_3Ph); 21.82 (s, CH_3CH); 22.03 (s, CH_3CH); 30.21 (s, *CH p*-cymene); 30.41 (s, CH_2Ph); 32.39 (d, $J = 27$, CH_2P); 68.60 (d, $J = 8$, Cp); 69.37 (s, Cp); 69.87 (d, $J = 7$, Cp); 70.49 (d, $J = 11$, Cp); 70.71 (d, $J = 8.8$, Cp); 83.89 (d, $J = 5$, *CH p*-cymene); 84.60 (d, $J = 6$, *CH p*-cymene); 89.90 (d, $J = 4$, *CH p*-cymene); 90.57 (d, $J = 5.5$, *CH p*-cymene); 92.76 (s, *p*-cymene); 107.15 (s, *p*-cymene); 125.86 (s, 2,6-Ph); 127.98 (s, 4-Ph); 138.28 (s, Ph); 141.88 (d, $J = 11.00$, 1-Ph); 159.81 (s, Ph). $^{31}\text{P}\{^1\text{H}\}$ NMR (101.2 MHz): δ (ppm) 9.4 (s). FT-IR: ν (cm^{-1}) 460; 848; 1080; 1104.06; 1280; 1383; 1466; 2867; 2914; 2960; 3083.

Dichloro(η^6 -*p*-cymene)[(R)-ferrocenyl(2-(2-naphthyl)methyl)methylphosphine]ruthenium(III) (6d). The phosphine was deprotected with method A. The preparation of this compound was carried out following the general protocol. The crude product was purified by flash chromatography (hexane/ethyl acetate, 9/1; $R_f = 0.25$) to obtain the title product as an orange solid in 90% yield. Anal. Calcd for $\text{C}_{33}\text{H}_{37}\text{RuCl}_2\text{PFe}$: C, 57.24; H, 5.38. Found: C, 57.9; H, 5.3. ^1H NMR (400 MHz): δ (ppm) 1.01 (d, $J = 8$, CH_3CH , 3H); 1.08 (d, $J = 8$, CH_3CH , 3H); 1.81 (s, CH_3 , *p*-cymene, 3H); 1.89 (d, $J = 12$, CH_3P , 3H); 2.62 (septet, $J = 8$, Me_2CH , 1H); 2.71 (m, CH_2P , 1H); 2.84 (m, CH_2P , 1H); 3.30 (m, CH_2Ar , 1H); 3.39 (m, CH_2Ar , 1H); 4.31 (s, Cp, 5H); 4.47 (s, Cp, 1H); 4.51 (s, Cp, 2H); 4.60 (s, Cp, 1H); 5.05 (d, $J = 8$, *p*-cymene 1H); 5.15 (s, *p*-cymene 2H); 5.20 (d, $J = 8$, *p*-cymene 1H); 7.41–4.50 (m, Ar, 3H); 7.75 (s, Ar, 1H); 7.80–7.86 (m, Ar, 3H). $^{13}\text{C}\{^1\text{H}\}$ NMR (100.6 MHz): δ (ppm) 9.50 (d, $J = 34.3$, CH_3P); 17.74 (s, CH_3 , *p*-cymene); 21.80 (s, CH_3CH); 21.99 (s, CH_3CH); 30.21 (s, *CH p*-cymene); 30.68 (s, CH_2Ar); 30.20 (d, $J = 28.30$, CH_2P); 68.65 (d, $J = 9.1$, Cp); 69.35 (s, Cp); 69.97 (d, $J = 7.07$, Cp); 70.32 (d, $J = 11.00$, Cp); 70.67 (d, $J = 8.08$, Cp); 84.03 (d, $J = 6.05$, *CH p*-cymene); 84.65 (d, $J = 6.05$, *CH p*-cymene); 90.16 (d, $J = 6.05$, *CH p*-cymene); 90.56 (d, $J = 6.05$, *CH p*-cymene); 92.73 (s, *p*-cymene); 107.15 (s, *p*-cymene); 125.44 (s); 126.12 (d, $J = 5.00$, Ar); 126.74 (s); 127.47 (s, Ar); 127.64 (s, Ar); 128.42 (s); 132.13 (s); 133.64 (s); 139.50 (d, $J = 13.10$, Ar); $^{31}\text{P}\{^1\text{H}\}$ NMR (101.2 MHz): δ (ppm) 10.5 (s). FT-IR: ν (cm^{-1}) 455; 487; 743; 821; 896; 1003; 1034; 1105; 1167; 1279; 1385; 1470; 1599; 1632; 2862; 2917; 2951; 3056.

Dichloro(η^6 -*p*-cymene)[(R)-ferrocenyl(2-(3-methoxyphenyl)ethyl)methylphosphine]ruthenium(III) (6e). The phosphine–borane was deprotected with method A. The preparation of this compound was carried out following the general protocol. The crude product was purified by flash chromatography (hexane/ethyl acetate, 9/1; $R_f = 0.15$) to obtain the title product as an orange foam in 90% yield. Anal. Calcd for $\text{C}_{30}\text{H}_{37}\text{RuCl}_2\text{PFeO}$: C, 53.59; H, 5.55. Found: C, 53.90; H, 5.50. ^1H NMR (400 MHz): δ (ppm) 0.98 (d, $J = 8$, CH_3CH , 3H); 1.06 (d, $J = 8$, CH_3CH , 3H); 1.77 (s, CH_3 , *p*-cymene, 3H); 1.83 (d, $J = 12$, CH_3P , 3H); 2.56–2.66 (m, *CH p*-cymene, 1H); 2.69–2.80 (m,

CH₂P, 2H); 3.05–3.22 (m, CH₂Ph, 2H); 3.82 (s, CH₃O, 3H); 4.28 (s, Cp, 5H); 4.43 (s, Cp, 1H); 4.48 (s, Cp, 2H); 4.57 (s, Cp, 1H); 5.01 (d, *J* = 4, *p*-cymene 1H); 5.13 (s, *p*-cymene 2H); 5.19 (d, *J* = 4, *p*-cymene 1H); 6.78 (d, *J* = 8, Ph, 1H); 6.86 (s, Ph, 1H); 6.89 (d, *J* = 8, Ph, 1H); 7.24–7.26 (m, Ph, 1H). ¹³C{¹H} NMR (100.6 MHz): δ (ppm) 9.29 (d, *J* = 34.4; CH₂P); 17.66 (s, CH₃ *p*-cymene); 21.74 (s, CH₃CH); 21.95 (s, CH₃CH); 30.17 (s, CH *p*-cymene); 30.46 (s, CH₂Ph); 32.14 (d, *J* = 27.3; CH₂P); 55.19 (s, CH₃O); 68.56 (d, *J* = 9.1; Cp); 69.29 (s, Cp); 69.90 (d, *J* = 7.7; Cp); 70.31 (d, *J* = 11; Cp); 70.65 (d, *J* = 8.8; Cp); 83.94 (d, *J* = 6.6; CH *p*-cymene); 84.55 (d, *J* = 6.60; CH *p*-cymene); 90.05 (d, *J* = 4.42; CH *p*-cymene); 90.57 (d, *J* = 5.50; CH *p*-cymene); 92.62 (s, *p*-cymene); 107.07 (s, *p*-cymene); 111.54 (s, Ph); 113.82 (s, 2-Ph); 120.26 (s, Ph); 129.68 (s, 5-Ph); 143.60 (d, *J* = 13, 1-Ph); 159.81 (s; 3-Ph). ³¹P{¹H} NMR (101.2 MHz): δ (ppm) 10.6 (s). FT-IR: ν (cm⁻¹) 452; 483; 690; 772; 823; 878; 1035; 1166; 1258; 1384; 1436; 1465; 1490; 1583; 1599; 2832; 2868; 2920; 2957; 3076.

Dichloro(η⁶-*p*-cymene)[(R)-ferrocenyl(2,2-dimethyl-3-phenyl-2-sila-1-propyl)methylphosphine]ruthenium(III) (6i). The phosphine was deprotected with method A. The preparation of this compound was carried out following the general protocol. The crude orange oil was crystallized from dichloromethane/hexane to obtain the title product as an orange powder in 90% yield. Anal. Calcd for C₃₁H₄₁Cl₂RuFePSi: C, 53.15; H, 5.90. Found: C, 52.49; H, 6.08. ¹H NMR (400 MHz): δ (ppm) 0.28 (s, CH₃Si, 3H); 0.32 (s, CH₃Si, 3H); 1.01 (d, *J* = 7.2, CH₃CH, 3H); 1.03 (d, *J* = 7.2, CH₃CH, 3H); 1.76 (s, CH₃ *p*-cymene, 3H); 1.76–1.79 (m, CH₃P, CH₂P, 5H); 2.24–2.37 (m, CH₃CH, 1H); 2.25 (d, *J* = 12.00, CH₂Si, 1H); 2.35 (d, *J* = 12.00, CH₂Si, 1H); 4.19 (s, Cp, 5H); 4.35 (s, Cp, 1H); 4.44 (s, Cp, 2H); 4.55 (s, Cp, 1H); 4.89 (d, *J* = 5.6, *p*-cymene, 1H); 5.03 (d, *J* = 5.6, *p*-cymene, 1H); 5.14 (d, *J* = 5.2, *p*-cymene, 1H); 5.24 (d, *J* = 5.6, *p*-cymene, 1H); 7.09–7.11 (m, Ph, 3H); 7.24–7.28 (m, Ph, 2H). ¹³C{¹H} NMR (100.6 MHz): δ (ppm) -0.08 (s, CH₃Si); 0.00 (s, CH₃Si); 13.74 (d, *J* = 36.22, CH₃P); 15.86 (d, *J* = 19.12, CH₂P); 17.87 (s, CH₃ *p*-cymene); 21.73 (s, CH₃CH); 22.60 (s, CH₃CH); 28.26 (d, *J* = 4.02, CH₂Si); 29.85 (d, *J* = 37, CH₃CH); 69.12 (Cp); 69.75 (d, *J* = 7, Cp); 70.24–70.44 (m, Cp); 84.53 (d, *J* = 5.03, CH *p*-cymene); 85.70 (d, *J* = 5.03, CH *p*-cymene); 87.95 (d, *J* = 4.02, CH *p*-cymene); 88.49 (d, *J* = 6.04, CH *p*-cymene); 95.69 (s, *p*-cymene); 106.32 (s, *p*-cymene); 124.26 (s, Ph); 128.26 (s, Ph); 128.32 (s, Ph); 139.93 (s, Ph). ³¹P{¹H} NMR (101.2 MHz): δ (ppm) 8.8 (s). FT-IR: ν (cm⁻¹) 482; 501; 700; 763; 826; 880; 1030; 1052; 1124; 1204; 1242; 1276; 1491; 1598; 2959; 3029; 3083.

Dichloro(η⁶-*p*-cymene)[(R)-ferrocenyl(2-methyl-2-phenyl-2-sila-1-propyl)methylphosphine]ruthenium(III) (6j). The phosphine-borane was deprotected with method B. The preparation of this compound was carried out following the general protocol. The crude orange oil was crystallized from dichloromethane/hexane to obtain the title product as an orange powder in 80% yield. Anal. Calcd for C₃₀H₃₉Cl₂PFeRuSi: C, 52.49; H, 5.73. Found: C, 52.21; H, 5.89. ¹H NMR (400 MHz): δ (ppm) 0.60 (s, CH₃Si, 3H); 0.64 (s, CH₃Si, 3H); 1.01 (d, *J* = 8, CH₃CH, 3H); 1.03 (d, *J* = 8, CH₃CH, 3H); 1.74 (d, *J* = 8, CH₃P, 3H); 1.75 (s, CH₃ *p*-cymene, 3H); 2.04 (d, *J* = 16, CH₂P, 2H); 2.38 (septet, *J* = 8, CH₃CH, 1H); 4.15 (s, Cp, 5H); 4.38 (s, Cp, 1H); 4.41 (s, Cp, 2H); 4.50 (s, Cp, 1H); 4.94 (d, *J* = 8, *p*-cymene, 1H); 5.00 (d, *J* = 4.1, *p*-cymene, 1H); 5.14 (d, *J* = 4.1, *p*-cymene, 1H); 5.22 (d, *J* = 4.1, *p*-cymene, 1H); 7.38–7.39 (m, Ph, 3H); 7.64–7.66 (m, *m*-Ph, 2H). ¹³C{¹H} NMR (100.6 MHz): δ (ppm) 0.13 (s, CH₃Si); 13.41 (d, *J* = 35.22, CH₃P); 17.68 (d, *J* = 21.13, CH₂P); 17.82 (s, CH₃ *p*-cymene); 21.82 (s, CH₃CH); 22.38 (s, CH₃CH); 30.07 (s, CH₃CH); 69.07 (s, Cp); 69.47 (d, *J* = 10, Cp); 69.74 (d, *J* = 8, Cp); 70.17 (d, *J* = 10, Cp); 70.26 (d, *J* = 9, Cp); 84.56 (d, *J* = 6, CH *p*-cymene); 85.27 (d, *J* = 5, CH *p*-cymene); 88.61 (d, *J* = 4, CH *p*-cymene); 88.96 (d, *J* = 6, CH *p*-cymene); 94.98 (s, *p*-cymene); 106.45 (s, *p*-cymene); 128.04 (s, Ph); 129.21 (s, Ph); 133.49 (s, Ph); 140.22 (s, Ph). ³¹P{¹H} NMR (101.2 MHz): δ (ppm) 9.2 (s). FT-IR: ν (cm⁻¹) 456; 502; 698; 725; 785; 821; 891; 1031; 1114; 1246; 1280; 1426; 1469; 2923; 2950; 3043; 3076; 3096.

Tethered [RuCl₂(κ-P*–η⁶-arene)] Complexes. General Procedure. A 1 mmol portion of the half-sandwich complex [RuCl₂(η⁶-

cymene)(P*)] was dissolved in 20 mL of chlorobenzene and the mixture stirred at 130 °C for 4 h. ³¹P NMR confirmed the quantitative formation of the tethered complex with total consumption of the starting product. The solution was cooled down slowly to 25 °C. The addition of 10 mL of hexane caused, after 10 min, the precipitation of the desired complex. The product was filtered and purified by crystallization from CH₂Cl₂/hexane.

Dichloro[κ-P-η⁶-(R)-tert-butyl(2-(3-phenylphenyl)ethyl)-methylphosphine]ruthenium(III) (7g). This compound was obtained as described in the general procedure, but starting from 0.117 g (0.193 mmol) of **4g**. Yield: 41 mg, 45%. Anal. Calcd for C₁₉H₂₅Cl₂PRu: C, 50.01; H, 5.52. Found: C, 49.8; H, 5.3.

¹H NMR (500.0 MHz, 298 K): major isomer, δ (ppm) 1.27 (d, *J*_{HP} = 14.7, (CH₃)₃C, 9H); 1.63 (d, *J*_{HP} = 10.5, CH₃P, 3H); 2.20–2.32 (m, CH₂Ph, 1H); 2.64–2.72 (m, CH₂P, 1H); 3.01–3.19 (m, CH₂P, CH₂Ph, 2H); 4.94 (s, Ar, 1H); 5.28 (d *J*_{HH} = 5.8, Ar, 1H), 5.80 (t, *J*_{HH} = 5.9, Ar, 1H); 6.26 (d, *J*_{HH} = 5.9, Ar, 1H); 7.41–7.51 (m, Ph, 3H); 7.68–7.74 (m, Ph, 2H); minor isomer, δ (ppm) 1.24 (d, *J*_{HP} = 14.8, (CH₃)₃C, 9H), 1.60 (d, *J*_{HP} = 10.6, CH₃P, 3H); 2.52–2.64 (m, CH₂Ph, 1H); 2.72–2.92 (m, CH₂P, CH₂Ph, 2H), 3.08–3.16 (m, CH₂P, 1H); 4.97 (d, *J*_{HH} = 5.4, Ar, 1H); 5.24 (s, Ar, 1H); 6.11 (t, *J*_{HH} = 5.9, Ar, 1H); 6.37 (d, *J*_{HH} = 6.3, Ar, 1H); 7.41–7.51 (m, Ph, 3H); 7.62–7.66 (m, Ph, 2H). ¹³C{¹H} NMR (100.6 MHz, 298 K, CDCl₃): major isomer, δ (ppm) 10.7 (d, *J*_{PC} = 25.6, PCH₃); 25.9 (d, *J*_{PC} = 2.5, C(CH₃)₃); 28.9 (d, *J*_{PC} = 3.35, CH₂Ph); 32.6 (d, *J*_{PC} = 22.1, C(CH₃)₃); 37.7 (d, *J*_{PC} = 27.9, CH₂P); 73.8 (s, CHAr); 75.3 (s, CHAr); 89.1 (d, *J*_{PC} = 13.1, CHAr); 95.2 (s, CHAr); 110.0 (d, *J*_{PC} = 4.04 Hz, CAr); 116.5 (d, *J* = 5.87 Hz, CAr); 129.5 (s, CPh); 130.1 (s, CPh); 133.6 (s, CPh); minor isomer: δ (ppm) 10.6 (d, *J*_{PC} = 25.6, PCH₃), 26.1 (d, *J*_{PC} = 2.40, C(CH₃)₃); 29.7 (d, *J*_{PC} = 3.9, CH₂Ph); 32.7 (d, *J*_{PC} = 21.4, C(CH₃)₃); 38.5 (d, *J*_{PC} = 27.6, CH₂P); 73.4 (s, CHAr), 76.4 (s, CHAr); 87.8 (d, *J*_{PC} = 14.0, CHAr); 98.5 (s, CHAr); 111.0 (d, *J*_{PC} = 4.09, CAr); 111.3 (d, *J* = 1.45, CAr); 129.6 (s, CHPh); 130.0 (s, CHPh). ³¹P{¹H} NMR (101.2 MHz, C₆H₅Cl, 298 K): δ (ppm) major isomer 63.6 (s), minor isomer 61.4 (s). X-ray: red crystals suitable for X-ray diffraction were obtained by slow diffusion of hexane over a solution of the complex in dichloromethane, at room temperature.

Dichloro[κ-P-η⁶-(R)-tert-butyl(2,2-dimethyl-3-phenyl-2-sila-1-propyl)methylphosphine]ruthenium(III) (7i). The preparation of this compound was carried out following the general protocol. The product was isolated as an orange solid in 90% yield. Anal. Calcd for C₁₄H₂₆Cl₂RuPSi: C, 39.53; H, 6.21. Found: C, 39.5; H, 6.1. ¹H NMR (400 MHz): δ (ppm) 0.29 (s, CH₃Si, 3H); 0.40 (s, CH₃Si, 3H); 1.02 (pt, *J* = 15, CH₂P, 1H); 1.12 (pt, *J* = 15.00, CH₂P, 1H); 1.27 (d, *J* = 14.10, C(CH₃)₃, 9H); 1.43 (d, *J* = 12, CH₃P, 3H); 1.63 (d, *J* = 15, CH₂Si, 1H); 1.86 (d, *J* = 15, CH₂Si, 1H); 5.07 (t, *J* = 5.4, Ph, 1H); 5.13 (d, *J* = 6, Ph, 1H); 5.35 (t, *J* = 4.8, Ph, 1H); 6.12 (t, *J* = 6, Ph, 1H); 6.23 (t, *J* = 5.7, Ph, 1H). ¹³C{¹H} NMR (100.6 MHz): δ (ppm) -1.04 (s, CH₃Si); -0.11 (d, *J* = 5, CH₃Si); 7.53 (d, *J* = 9.06, CH₂P); 10.1 (d, *J* = 30.2, CH₃P); 18.28 (s, CH₂Si); 27.92 (s, C(CH₃)₃); 35.18 (d, *J* = 25.15, C(CH₃)₃); 79.54 (s, Ph); 79.91 (s, Ph); 86.42 (s, Ph); 95.46 (d, *J* = 10.62, Ph); 96.58 (s, Ph); 101.48 (d, *J* = 11.1, Ph). ³¹P{¹H} NMR (101.2 MHz): δ (ppm) 32.53 (s). FT-IR: ν (cm⁻¹) 809; 839; 897; 1102; 1251; 1448; 1464; 2864; 2897; 2947; 3057.

Dichloro[κ-P-η⁶-(R)-tert-butyl(2-methyl-2-phenyl-2-sila-1-propyl)-methylphosphine]ruthenium(III) (7j). The preparation of this compound was carried out following the general protocol. The product was isolated as an orange solid in 90% yield. Anal. Calcd for C₁₄H₂₅Cl₂PRuSi: C, 39.62; H, 5.94. Found: C, 39.5; H, 5.9. ¹H NMR (400 MHz): δ (ppm) 0.46 (s, CH₃Si, 3H); 0.54 (s, CH₃Si, 3H); 1.23 (d, *J* = 15.00, C(CH₃)₃, 9H); 1.49 (d, *J* = 10.8, CH₃P, 3H); 1.66 (pt, *J* = 14.5, CH₂, 1H); 2.09 (dd, *J* = 14.6, *J* = 10.7, CH₂, 1H); 5.19 (d, *J* = 5.3, Ph, 1H); 5.35 (d, *J* = 4.3, Ph, 1H); 5.52 (t, *J* = 5.7, Ph, 1H); 6.07 (t, *J* = 6, Ph, 1H); 6.19 (t, *J* = 6, Ph, 1H). ¹³C{¹H} NMR (100.6 MHz): δ (ppm) -3.92 (d, *J* = 7.04, CH₃Si); -2.08 (d, *J* = 8.05, CH₃Si); 11.53 (d, *J* = 27.16, CH₃P); 21.79 (d, *J* = 12.07, CH₂P); 26.28 (d, *J* = 3.0, C(CH₃)₃); 34.30 (d, *J* = 21.13, C(CH₃)₃); 82.40 (s, Ph); 86.35 (s, Ph); 88.53 (s, Ph); 96.76 (d, *J* = 9.05, Ph); 98.67 (d, *J* = 10.00, Ph). ³¹P{¹H} NMR (101.2 MHz): δ (ppm) 32.88 (s). FT-IR: ν

(cm^{-1}) 425; 753; 794; 812; 848; 888; 1013; 1096; 1256; 1280; 1364; 1392; 1463; 1637; 2882; 2944; 3025.

Dichloro[κ -P- η^6 -(R)-tert-butyl(2,2-diphenylethyl)-methylphosphine]ruthenium(II) (7I). This compound was obtained as described in the general procedure, but starting from 0.117 g (0.198 mmol) of **4I**. Yield: 41 mg, 45%. Anal. Calcd for $\text{C}_{19}\text{H}_{25}\text{Cl}_2\text{PRu}$: C, 50.01; H, 5.52. Found: C, 50.2; H, 5.3.

^1H NMR (500.0 MHz, 298 K): major isomer, δ (ppm) 1.37 (d, $J_{\text{HP}} = 15.0$, $(\text{CH}_3)_3\text{C}$, 9H); 1.64 (d, $J_{\text{HP}} = 10.9$, CH_3P , 3H); 3.18 (ptd, $J = 11.3$, $J = 8.4$, CH_2P , 1H); 3.47–3.55 (m, CH_2P , 1H); 4.01 (ddd, $J = 13.9$, $J = 6.0$, $J = 1.5$, CHPh_2 , 1H); 5.00 (d, $J = 5.9$, Ar, 1H); 5.31 (d, $J = 5.9$, Ar, 1H); 5.81 (t, $J = 5.8$, Ar, 1H); 6.08 (t, $J = 5.9$, Ar, 1H); 6.25 (td, $J = 6.0$, $J = 2.6$, Ar, 1H); 7.30–7.41 (m, Ph, 5H) minor isomer, δ (ppm) 1.31 (d, $J_{\text{HP}} = 15.2$, $(\text{CH}_3)_3\text{C}$, 9H); 1.76 (d, $J_{\text{HP}} = 10.5$, CH_3P , 3H); 3.02 (ddd, $J = 13.7$, $J = 11.7$, $J = 5.6$, CH_2P , 1H); 3.41–3.48 (m, CH_2P , 1H); 3.83 (ddd, $J = 13.7$, $J = 5.5$, $J = 1.7$, CHPh_2 , 1H); 5.02 (d, $J = 5.4$, Ar, 1H); 5.27 (d, $J = 6.0$, Ar, 1H); 5.72 (t, $J = 5.7$, Ar, 1H); 6.16 (td, $J = 5.9$, $J = 2.0$, Ar, 1H); 6.31 (t, $J = 5.7$, Ar, 1H); 7.30–7.41 (m, Ph, 5H). $^{13}\text{C}\{^1\text{H}\}$ NMR (100.6 MHz, 298 K, CDCl_3): major isomer, δ (ppm) 11.5 (d, $J_{\text{PC}} = 27.8$, PCH_3); 26.7 (d, $J_{\text{PC}} = 2.85$, $\text{C}(\text{CH}_3)_3$); 33.1 (d, $J_{\text{PC}} = 20.1$, $\text{C}(\text{CH}_3)_3$); 44.3 (d, $J_{\text{PC}} = 27.0$, CH_2P); 49.6 (d, $J_{\text{PC}} = 3.35$, CHPh_2); 73.8 (s, CHAr); 77.9 (s, CHAr); 91.2 (d, $J_{\text{PC}} = 13.4$, CHAr); 95.4 (s, CHAr); 102.5 (d, $J_{\text{PC}} = 4.63$, CHAr); 112.8 (d, $J_{\text{PC}} = 2.12$, CAr); 126.7 (s, Ph); 128.1 (s, Ph); 129.1 (s, Ph); minor isomer, δ (ppm) 10.0 (d, $J_{\text{PC}} = 25.1$, PCH_3); 25.8 (d, $J_{\text{PC}} = 2.28$, $\text{C}(\text{CH}_3)_3$); 32.6 (d, $J_{\text{PC}} = 21.9$, $\text{C}(\text{CH}_3)_3$); 41.9 (d, $J_{\text{PC}} = 27.1$, CH_2P); 45.3 (d, $J_{\text{PC}} = 6.02$, CHPh_2); 73.7 (s, CHAr); 77.2 (s, CHAr); 89.3 (d, $J_{\text{PC}} = 14.5$, CHAr); 94.8 (s, $\text{C}_{\text{ar}}\text{H}$); 101.8 (d, $J_{\text{PC}} = 6.10$, CHAr); 110.3 (d, $J_{\text{PC}} = 2.37$, CAr); 126.8 (s, Ph); 128.1 (s, Ph); 129.2 (s, Ph). $^{31}\text{P}\{^1\text{H}\}$ NMR (101.2 MHz, 298 K), major isomer δ (ppm) 47.2 (s), minor isomer δ (ppm) 45.1. X-ray: red crystals suitable for X-ray diffraction were obtained by slow diffusion of hexane over a solution of the complex in chlorobenzene, at room temperature.

Dichloro[κ -P- η^6 -(R)-cyclohexyl(2-dimethylbenzylsilyl)-methylphosphine]ruthenium(II) (8i). The preparation of this compound was carried out following the general protocol. The product was isolated as an orange solid in 90% yield. Monocrystals of the title product were obtained after slow evaporation from a solution of dichloromethane/hexane. Anal. Calcd for $\text{C}_{17}\text{H}_{29}\text{Cl}_2\text{PRuSi}$: C, 43.96; H, 6.29. Found: C, 42.1; H, 6.25. ^1H NMR (400 MHz): δ (ppm) 0.32 (s, CH_3Si , 3H); 0.34 (s, CH_3Si , 3H); 1.15 (d, $J = 14.8$, CH_2P , 2H); 1.15–1.33 (m, Cy, 6H); 1.37 (d, $J = 11.2$, CH_3P , 3H); 1.66 (d, $J = 12$, CH_2Ar , 1H); 1.80–1.95 (m, Cy, 4H); 1.96 (d, $J = 12$, CH_2Si , 1H); 2.05 (m, CHP , 1H); 4.87 (d, $J = 5.60$, Ph, 1H); 4.94 (t, $J = 3.60$, Ph, 1H); 5.07 (t, $J = 5.20$, Ph, 1H); 6.15 (t, $J = 5.60$, Ph, 1H); 6.24 (t, $J = 5.60$, Ph, 1H). $^{13}\text{C}\{^1\text{H}\}$ NMR (100.6 MHz): δ (ppm) –0.62 (d, $J = 23.14$, CH_3Si); 0.14 (d, $J = 4.03$, CH_3Si); 6.03 (d, $J = 12.73$, CH_2P); 7.86 (d, $J = 32.10$, CH_2P); 18.24 (s, CH_2Ph); 26.12 (s, Cy); 26.95 (d, $J = 11$, Cy); 27.07 (d, $J = 12$, Cy); 27.53 (s, Cy); 27.84 (d, $J = 3$, Cy); 39.25 (d, $J = 33.1$, CHP); 79.38 (s, CHPh); 81.98 (s, CHPh); 83.01 (s, CHPh); 97.58 (s, CPh); 97.75 (d, $J = 10.6$, CHPh); 98.57 (d, $J = 10.1$, CHPh). $^{31}\text{P}\{^1\text{H}\}$ NMR (101.2 MHz): δ (ppm) 30.21. FT-IR: ν (cm^{-1}) 647; 737; 782; 808; 837; 897; 1098; 1173; 1200; 1251; 1405; 1446; 1508; 2850; 2923; 3056.

Dichloro[κ -P- η^6 -(R)-cyclohexyl(2-methyl-2-phenyl-2-sila-1-propyl)methylphosphine]ruthenium(II) (8j). The preparation of this compound was carried out following the general protocol. The product was isolated as an orange solid in 90% yield. Anal. Calcd for $\text{C}_{16}\text{H}_{27}\text{Cl}_2\text{PRuSi}$: C, 42.67; H, 6.04. Found: C, 43.6; H, 6.1. ^1H NMR (400 MHz): δ (ppm) 0.46 (s, CH_3Si , 3H); 0.56 (s, CH_3Si , 3H); 1.20–2.30 (m, Cy, CH_2P , 13H); 1.47 (d, $J = 12.50$, CH_3P , 3H); 5.14 (d, $J = 8$, Ph 1H); 5.28 (d, $J = 8$, Ph 1H); 5.40 (t, $J = 7$, Ph, 1H); 6.05 (t, $J = 8$, Ph, 1H); 6.28 (t, $J = 8$, Ph, 1H). $^{13}\text{C}\{^1\text{H}\}$ NMR (100.6 MHz): δ (ppm) –3.78 (s, CH_3Si); –2.01 (d, $J = 8.35$, CH_3Si); 10.74 (d, $J = 29.17$, CH_2P); 20.98 (d, $J = 12.37$, CH_2P); 26.08 (s, Cy); 26.50 (s, Cy); 26.60 (s, Cy); 26.67 (s, Cy); 27.72 (s, Cy); 36.04 (d, $J = 25.95$, CHP); 81.54 (s, CHPh); 86.13 (s, CHPh); 87.14 (s, CHPh); 91.1 (s, CPh); 97.64 (d, $J = 11.07$, CHPh); 98.07 (d, $J = 9.46$, CHPh). $^{31}\text{P}\{^1\text{H}\}$ NMR (101.2 MHz): δ (ppm) 32.84 (s). FT-IR: ν (cm^{-1}) 728; 794;

816; 844; 878; 894; 920; 1090; 1117; 1252; 1279; 1447; 2849; 2924; 3056.

Dichloro[κ -P- η^6 -(R)-tert-butyl(2-(2,3,4,5,6-pentamethylphenyl)-ethyl)phosphine]ruthenium(II) (1c). X-ray: red crystals suitable for X-ray diffraction were obtained by slow diffusion of hexane over a solution of the complex **1c** prepared previously in chlorobenzene, at room temperature.⁹

General Procedure for the Enantioselective Transfer Hydrogenation. A typical transfer hydrogenation run was performed as follows. A 50 mL Schlenk flask was charged with the ruthenium precursor (0.02 mmol) and potassium *tert*-butoxide (11.2 mg, 0.1 mmol) and was purged with three vacuum/argon cycles. Under a gentle flow of argon, 25 mL of degassed 2-propanol was added and the flask heated to reflux (82 °C) for 30 min. After that time acetophenone (600 mg, 4.0 mmol) was rapidly added to start the catalytic run. The reaction was monitored by GC analysis.

■ ASSOCIATED CONTENT

Supporting Information

Text, tables, figures, and CIF files giving details of the synthesis of the *P*-stereogenic phosphines and molecular structure information, NMR spectra of selected phosphines and complexes, HPLC of selected phosphines, structural and electrochemical data of ruthenium complexes, time dependence of hydrogen transfer, techniques used to evaluate the anticancer activity, and crystallographic data. This material is available free of charge via the Internet at <http://pubs.acs.org>. CCDC 916123–916131 contain supplementary crystallographic data for this paper. These data can be obtained free of charge from The Cambridge Crystallographic Data Centre via www.ccdc.cam.ac.uk/data_request/cif.

■ AUTHOR INFORMATION

Notes

The authors declare no competing financial interest.

■ ACKNOWLEDGMENTS

We thank the Ministerio of Educación y Ciencia, (MEC, grant number CTQ2010-15292/BQU CTQ2008-02064) and BIO2007-6846-C02-01) for financial support of this work. Financial support from MEC (FPI 2008-002758) and the Consiglio Nazionale delle Ricerche and Regione Autonoma della Sardegna (Master and Back 2.2-139, PRR-MAB-A2011-19282) are gratefully acknowledged by A.M. R.A. thanks the DURSI of the Autonomous Government of Catalonia for the award of a Ph.D. grant.

■ REFERENCES

- (1) (a) Noyori, R. *Angew. Chem., Int. Ed.* **2002**, *41*, 2008–2022. (b) Grubbs, R. H. *Angew. Chem., Int. Ed.* **2006**, *45*, 3760–3765. (c) Trost, B. M.; Fredericksen, M. U.; Rudd, M. T. *Angew. Chem., Int. Ed.* **2006**, *45*, 6630–6666. (d) Ritleng, V.; Sirlin, C.; Pfeffer, M. *Chem. Rev.* **2002**, *102*, 1731–1769.
- (2) Murahashi, S.-I. *Ruthenium in Organic Synthesis*; Wiley-VCH: Weinheim, Germany, 2004.
- (3) (a) Süß-Fink, G.; Faure, M.; Ward, T. R. *Angew. Chem., Int. Ed.* **2002**, *41*, 99–101. (b) Severin, K. *Coord. Chem. Rev.* **2003**, *245*, 3–10. (c) Govindaswamy, P.; Linder, D.; Lacour, J.; Süß-Fink, G.; Therrien, B. *Chem. Commun.* **2006**, 4691–4693. (d) Severin, K. *Chem. Commun.* **2006**, 3859–3867. (e) Rauchfuss, T. B.; Severin, K. In *Organic Nanostructures*; Atwood, J. W., Steed, J. W., Eds.; Wiley-VCH: Weinheim, Germany, 2008; pp 179–203. (f) Therrien, B. *Eur. J. Inorg. Chem.* **2009**, 2445–2453.
- (4) (a) Hartinger, C. G.; Metzler-Nolte, N.; Dyson, P. J. *Organometallics* **2012**, *31*, 5677–5685. (b) Betanzos-Lara, S.; Salassa, L.; Habtemariam, A.; Novakova, O.; Pizarro, A. M.; Clarkson, G. J.;

- Liskova, B.; Brabec, V.; Sadler, P. J. *Organometallics* **2012**, *31*, 3466–3479. (c) Liu, H.-K.; Sadler, P. J. *Acc. Chem. Res.* **2011**, *44*, 349–359. (d) Smith, G. S.; Therrien, B. *Dalton Trans.* **2011**, *40*, 10793–10800. (e) Süß-Fink, G. *Dalton Trans.* **2010**, *39*, 1673–1688. (f) Hartinger, C. G.; Dyson, P. J. *Chem. Soc. Rev.* **2009**, *38*, 391–401. (g) Bruijninx, P. C. A.; Sadler, P. J. *Adv. Inorg. Chem.* **2009**, *61*, 1–62. (h) Peacock, A. F. A.; Sadler, P. J. *Chem. Asian J.* **2008**, *3*, 1890–1899. (i) Ang, W. H.; Dyson, P. J. *Eur. J. Inorg. Chem.* **2006**, 4003–4018. (j) Clarke, M. J. *Coord. Chem. Rev.* **2003**, *236*, 209–/233.
- (5) (a) Ganter, C. *Chem. Soc. Rev.* **2003**, *32*, 130–138. (b) Bauer, E. B. *Chem. Soc. Rev.* **2012**, *41*, 3153–3167.
- (6) Recent mechanistic studies: (a) Dinda, S.; Sebastian, K. L.; Samuelson, A. G. *Organometallics* **2010**, *29*, 6209–6218. (b) Chaplin, A. B.; Fellay, C.; Laurenczy, G.; Dyson, P. J. *Organometallics* **2007**, *26*, 586–593. (c) Arena, C. G.; Calamia, S.; Faraone, F.; Graiff, C.; Tiripicchio, A. *Dalton Trans.* **2000**, 3149–3157.
- (7) (a) Bennett, M. A. *Coord. Chem. Rev.* **1997**, *166*, 225–254. (b) Chatani, N. *Sci. Synth.* **2002**, *1*, 931–972. (c) Adams, J. R.; Bennett, M. A. *Adv. Organomet. Chem.* **2006**, *54*, 293–331. (d) Therrien, B. *Coord. Chem. Rev.* **2009**, *253*, 493–519.
- (8) (a) Brunner, H. *Eur. J. Inorg. Chem.* **2001**, 905–912. (b) Ward, T. R.; Schafer, O.; Daul, C.; Hofmann, P. *Organometallics* **1997**, *16*, 3207–3215. (c) Trost, B. M.; Vidal, B.; Thommen, M. *Chem. Eur. J.* **1999**, *5*, 1055–1069.
- (9) Aznar, R.; Muller, G.; Sainz, D.; Font-Bardia, M.; Solans, X. *Organometallics* **2008**, *27*, 1967–1969.
- (10) Muci, A. R.; Campos, K. R.; Evans, D. A. *J. Am. Chem. Soc.* **1995**, *117*, 9075–9076.
- (11) (a) Pietrusiewicz, K. M.; Zablocka, M. *Chem. Rev.* **1994**, *94*, 1375–1411. (b) Grabulosa, A.; Granell, J.; Muller, G. *Coord. Chem. Rev.* **2007**, *251*, 25–90. (c) Glueck, D. S. *Synlett* **2007**, 2627–2634. (d) Grabulosa, A. *P-Stereogenic Ligands in Enantioselective Catalysis; Royal Society of Chemistry: Cambridge, U.K.*, 2011.
- (12) Hoppe, D.; Hense, T. *Angew. Chem., Int. Ed. Engl.* **1997**, *36*, 2282–2316.
- (13) Strohmman, C.; Strohfeltd, K.; Schildbach, D. *J. Am. Chem. Soc.* **2003**, *125*, 13672–13673 and references therein.
- (14) (a) Imamoto, T.; Watanabe, J.; Wada, Y.; Masuda, H.; Yamada, H.; Tsuruta, H.; Matsukawa, S.; Yamaguchi, K. *J. Am. Chem. Soc.* **1998**, *120*, 1635. (b) Johansson, M. J.; Schwartz, L. O.; Oohara, N.; Katagiri, K.; Imamoto, T. *Tetrahedron: Asymmetry* **2003**, *14*, 2171–2175. (c) Amedjkouh, M.; Kann, N. C. *Eur. J. Org. Chem.* **2004**, 1894–1896. (d) Dolhem, F.; Johansson, M.; Antosson, T.; Kann, N. *J. Comb. Chem.* **2007**, 477–486. (e) Morisaki, Y.; Imoto, H.; Tsurui, K.; Chujo, Y. *Org. Lett.* **2009**, *11*, 2244.
- (15) (a) Johansson, M. J.; Schwartz, L. O.; Amedjkouh, M.; Kann, N. C. *Tetrahedron: Asymmetry* **2004**, *15*, 3531–3538. (b) McGrath, M. J.; O'Brien, P. *J. Am. Chem. Soc.* **2005**, *127*, 16378–16379. (c) Stead, D.; O'Brien, P.; Sanderson, A. *Org. Lett.* **2008**, *10*, 1409–1412.
- (16) Gammon, J. J.; O'Brien, P.; Kelly, B. *Org. Lett.* **2009**, *11*, 5022–5025.
- (17) (a) Gammon, J. J.; Canipa, S. J.; O'Brien, P.; Kelly, B.; Taylor, S. *Chem. Commun.* **2008**, 3750–3752. (b) Canipa, S. J.; O'Brien, P.; Taylor, S. *Tetrahedron: Asymmetry* **2009**, *20*, 2407–2412. (c) Granander, J.; Secci, F.; Canipa, S. J.; O'Brien, P.; Kelly, B. *J. Org. Chem.* **2011**, *76*, 4794–4799.
- (18) Grabulosa, A.; Mannu, A.; Muller, G.; Calvet, T.; Font-Bardia, M. *J. Organomet. Chem.* **2011**, *696*, 2338–2345.
- (19) Gessner, V. H.; Dilsky, S.; Strohmman, C. *Chem. Commun.* **2010**, 46, 4719–4721.
- (20) Carbone, G.; O'Brien, P.; Hilmersson, G. *J. Am. Chem. Soc.* **2010**, *132*, 15455–15450.
- (21) (a) Heath, H.; Wolfe, B.; Livinghouse, T.; Bae, S. K. *Synthesis* **2001**, 2341–2347. (b) Wolfe, B.; Livinghouse, T. *J. Org. Chem.* **2001**, *66*, 1514–1516.
- (22) Colby, E. A.; Jamison, T. F. *J. Org. Chem.* **2003**, *68*, 156–166.
- (23) (a) Gatineau, D.; Giordano, L.; Buono, G. *J. Am. Chem. Soc.* **2011**, *133*, 10728–10731. (b) Wawrzyniak, P.; Kindermann, M. K.; Heinicke, J. W.; Jones, P. G. *Eur. J. Org. Chem.* **2011**, 593–606.
- (c) Kumaraswamy, G.; Rao, G. V.; Murthy, A. N.; Sridhar, B. *Synlett* **2009**, 1180–1184. (d) Takahashi, Y.; Yamamoto, Y.; Katagiri, K.; Danjo, H.; Yamaguchi, K.; Imamoto, T. *J. Org. Chem.* **2005**, *70*, 9009–9012. (e) Nagata, K.; Matsukawa, S.; Imamoto, T. *J. Org. Chem.* **2000**, *65*, 4185–4188.
- (24) (a) Imamoto, T.; Kusumoto, T.; Suzuki, N.; Sato, K. *J. Am. Chem. Soc.* **1985**, *107*, 5301–5303. (b) Imamoto, T.; Oshiki, T.; Onozawa, T.; Kusumoto, T.; Sato, K. *J. Am. Chem. Soc.* **1990**, *112*, 5244–5252. (c) Brisset, H.; Gourdel, Y.; Pellon, P.; Le Corre, M. *Tetrahedron Lett.* **1993**, *34*, 4523–4526. (d) Bradley, D.; Williams, G.; Lombard, H.; Van Niekerk, M.; Coetzee, P. P. *Phosphorus, Sulfur Silicon Relat. Elem.* **2002**, *177*, 2115–2116.
- (25) Sayalero, S.; Pericàs, M. A. *Synlett* **2006**, 2585–2588.
- (26) (a) McKinstry, L.; Livinghouse, T. *Tetrahedron Lett.* **1994**, *35*, 9319–9322. (b) McKinstry, L.; Livinghouse, T. *Tetrahedron* **1995**, *51*, 7655–7666. (c) McKinstry, L.; Overberg, J. J.; Soubra-Ghaoui, C.; Walsh, D. S.; Robins, K. A. *J. Org. Chem.* **2000**, *65*, 2261–2263.
- (27) (a) M. Schroder, M.; Nozaki, K.; Hiyama, T. *Bull. Chem. Soc. Jpn.* **2004**, *77*, 1931–1932. (b) van Overschelde, M.; Verdecken, E.; Modha, S. G.; Cogen, S.; van der Eycken, E.; van der Eycken, J. *Tetrahedron* **2009**, *65*, 6410–6415.
- (28) (a) Chooi, S. Y. M.; Leung, P.-H.; Lim, C. C.; Mok, K. F.; Quek, G. H.; Sim, K. Y.; Tan, M. K. *Tetrahedron: Asymmetry* **1992**, *3*, 529–532. (b) Albert, J.; Granell, J.; Muller, G.; Sainz, D. *Tetrahedron: Asymmetry* **1995**, *6*, 325–328. (c) Dunina, V. V.; Kuz'mina, L. G.; Kazakova, M. Y.; Grishin, Y. K.; Veits, Y. A.; Kazakova, E. I. *Tetrahedron: Asymmetry* **1997**, *8*, 2537–2545. (d) Albert, J.; Granell, J.; Muller, G. *J. Organomet. Chem.* **2007**, *691*, 2101–2006.
- (29) Albert, J.; Cadena, J. M.; Granell, J. *Tetrahedron: Asymmetry* **1997**, *8*, 991–994.
- (30) (a) Pinnell, R. P.; Megerle, C. A.; Manatt, S. L.; Kroon, P. A. *J. Am. Chem. Soc.* **1973**, *95*, 977–978. (b) Allen, D. W.; Taylor, B. F. *J. Chem. Soc., Dalton Trans.* **1982**, 51–54.
- (31) Muller, A.; Otto, S.; Roodt, A. *Dalton Trans.* **2008**, 650–657.
- (32) Tolman, C. A. *Chem. Rev.* **1977**, *77*, 313–348.
- (33) (a) Barnard, T. S.; Mason, M. R. *Organometallics* **2001**, *20*, 206–214. (b) Suarez, A.; Rojas, M.; Pizzano, A. *Organometallics* **2002**, *21*, 4611–4621. (c) van der Vlugt, J. I.; van Duren, R.; Batema, G. D.; van Heeten, R.; Meestma, A.; Fraanje, J.; Goubitz, K.; Kamer, P. C. J.; van Leeuwen, P. W. N. M.; Vogt, D. *Organometallics* **2005**, *24*, 5377–5382.
- (34) Carr, S. W.; Colton, R. *Aust. J. Chem.* **1981**, *34*, 35–44.
- (35) Hrib, C. G.; Ruthe, F.; Seppälä, E.; Bätcher, M.; Druckenbrodt, C.; Wismach, C.; Jones, P. G.; du Mont, W.-W.; Lippolis, V.; Devillanova, F. A.; Bühl, M. *Eur. J. Inorg. Chem.* **2006**, 88–100.
- (36) Smith, P.-D.; Wright, A. H. *J. Organomet. Chem.* **1998**, *559*, 141–147.
- (37) (a) Pinto, P.; Marconi, G.; Heinemann, F. W.; Zenneck, U. *Organometallics* **2004**, *23*, 374–380. (b) Weber, I.; Heinemann, F. W.; Bauer, W.; Superchi, S.; Zahl, A.; Richter, D.; Zenneck, U. *Organometallics* **2008**, *27*, 4116–4125. (c) Abele, A.; Wursche, R.; Klinga, M.; Rieger, B. *J. Mol. Catal. A: Chem.* **2000**, *160*, 23–33. (d) Huber, D.; Kumar, P. G. A.; Pregosin, P. S.; Mikhel, I. S.; Mezzetti, A. *Helv. Chim. Acta* **2006**, *89*, 1696–1714.
- (38) (a) Faller, J. W.; D'Alliessi, D. G. *Organometallics* **2003**, *22*, 2749–2757. (b) Faller, J. W.; Fontaine, P. P. *Organometallics* **2005**, *24*, 4132–4138. (c) Faller, J. W.; Fontaine, P. P. *Organometallics* **2007**, *26*, 1738–1743. (d) Therrien, B.; Ward, T. R.; Pilkington, M.; Hoffmann, C.; Gilardoni, F.; Weber, J. *Organometallics* **1998**, *17*, 330–337. (e) Therrien, B.; Ward, T. R. *Angew. Chem., Int. Ed.* **1999**, *38*, 405–408.
- (39) Pinto, P.; Götz, A. W.; Marconi, G.; Hess, B. A.; Marinetti, A.; Heinemann, F. W.; Zenneck, U. *Organometallics* **2006**, *25*, 2607–2616.
- (40) (a) Morris, D. J.; Hayes, A. M.; Wills, M. J. *Org. Chem.* **2006**, *71*, 7035–7044. (b) Geldbach, T. J.; Laurenczy, G.; Scopellini, R.; Dyson, P. J. *Organometallics* **2006**, *25*, 733–742. (c) Miyaki, Y.; Onishi, T.; Kurosawa, H. *Inorg. Chim. Acta* **2000**, *300–302*, 369–377.
- (41) Ito, M.; Endo, Y.; Ikariya, T. *Organometallics* **2008**, *27*, 6053–6055.

(42) (a) Umezawa-Vizzini, K.; Guzman-Jimenez, I. Y.; Whitmire, K. H.; Lee, T. R. *Organometallics* **2003**, *22*, 3059–3065. (b) Ghebreyessus, K. Y.; Nelson, J. H. *Inorg. Chim. Acta* **2003**, *350*, 12–24. (c) Bennett, M. A.; Edwards, A. J.; Harper, J. R.; Khimyak, T.; Willis, A. C. *J. Organomet. Chem.* **2001**, *629*, 7–18. (d) Therrien, B.; Ward, T. R.; Pilkington, M.; Hoffmann, C.; Gilardoni, F.; Weber, J. *Organometallics* **1998**, *17*, 330–337. (e) Ghebreyessus, K. Y.; Nelson, J. H. *Organometallics* **2000**, *19*, 3387–3392.

(43) (a) Zassinovich, G.; Mestroni, G.; Gladiali, S. *Chem. Rev.* **1992**, *92*, 1051–1089. (b) Gladiali, S.; Alberico, E. *Chem. Soc. Rev.* **2006**, *35*, 226–236. (c) Samec, J. S. M.; Bäckvall, J. E.; Andersson, P. G.; Brandt, P. *Chem. Soc. Rev.* **2006**, *35*, 237–248. (d) Parekh, V.; Ramsden, J. A.; Wills, M. *Catal. Sci. Technol.* **2012**, *2*, 406–414.

(44) (a) Bennett, M. A.; Smith, A. K. *J. Chem. Soc., Dalton Trans.* **1974**, 233–241. (b) Carriedo, G. A.; Crochet, P.; García Alonso, F. J.; Gimeno, J.; Presa-Soto, A. *Eur. J. Inorg. Chem.* **2004**, 3668–3674. (c) Wang, L.; Yang, Q.; Fu, H.-Y.; Chen, H.; Yuan, M.-L.; Li, R.-X. *Appl. Organomet. Chem.* **2011**, *25*, 626–631.

(45) (a) Grabulosa, A.; Mannu, A.; Mezzetti, A.; Muller, G. *J. Organomet. Chem.* **2012**, *696*, 4221–4228. (b) Grabulosa, A.; Mannu, A.; Alberico, E.; Denurra, S.; Gladiali, S.; Muller, G. *J. Mol. Catal. A: Chem.* **2012**, *363–364*, 49–57.

(46) (a) Solari, E.; Gauthier, S.; Scopelliti, R.; Severin, K. *Organometallics* **2009**, *28*, 4519–4526. (b) Chaplin, A. B.; Dyson, P. J. *Organometallics* **2007**, *26*, 4357–4360. (c) Demerseman, B.; Diagne, M.; Semeril, D.; Toupet, L.; Bruneau, C.; Dixneuf, P. H. *Eur. J. Inorg. Chem.* **2006**, 1174–1181. (d) Diez, J.; Gamasa, M. P.; Lastra, E.; Garcia-Fernandez, A.; Tarazona, M. P. *Eur. J. Inorg. Chem.* **2006**, 2855–2864. (e) Crochet, P.; Fernandez-Zumel, M. A.; Beauquis, C.; Gimeno, J. *Inorg. Chim. Acta* **2003**, *356*, 114–120. (f) Loges, B.; Boddien, A.; Junge, H.; Noyes, J. R.; Baumann, W.; Beller, M. *Chem. Commun.* **2009**, 4185–4187.

(47) DePasquale, J.; Kumar, M.; Zeller, M.; Papish, E. T. *Organometallics* **2013**, *32*, 966–979.

(48) (a) Melchart, M.; Habtemariam, A.; Novakova, O.; Moggach, F. P. A.; Fabbiani, F. P. A.; Parsons, S.; Brabec, V.; Sadler, P. J. *Inorg. Chem.* **2007**, *46*, 8950–8962. (b) Pizarro, A. M.; Melchart, M.; Habtemariam, A.; Salassa, L.; Fabbiani, F. P. A.; Parsons, S.; Sadler, P. J. *Inorg. Chem.* **2010**, *49*, 3310–3319. (c) Kilpin, K. J.; Clavel, C. M.; Edafe, F.; Dyson, P. J. *Organometallics* **2012**, *31*, 7031–7039.

(49) Fuertes, M. A.; Alonso, C.; Pérez, J. M. *Chem. Rev.* **2003**, *103*, 645–662.

(50) Perrin, D. D.; Armarego, W. *Purification of Laboratory Chemicals*; Butterworth Heinemann: Oxford, U.K., 2002.